CHAPTER IV

EXPERIMENTAL RESULTS OF AN UNSTEADY STATE HEAT PIPE

4.1 Experimental Apparatus

The test rig used in this study is shown diagramatically in Fig. 4.2. The rig has the following features and facilities:

(i) Heat for evaporator section (Fig.4.1)

Dimension of heater used

Outside diameter	7.2	cm.
Inside diameter	2.6	cm.
Length	14	cm.
Weight	830	gm.
Number of heater coils used	2	(2x1,000 W)
Geometrical type of heater	cylinder	

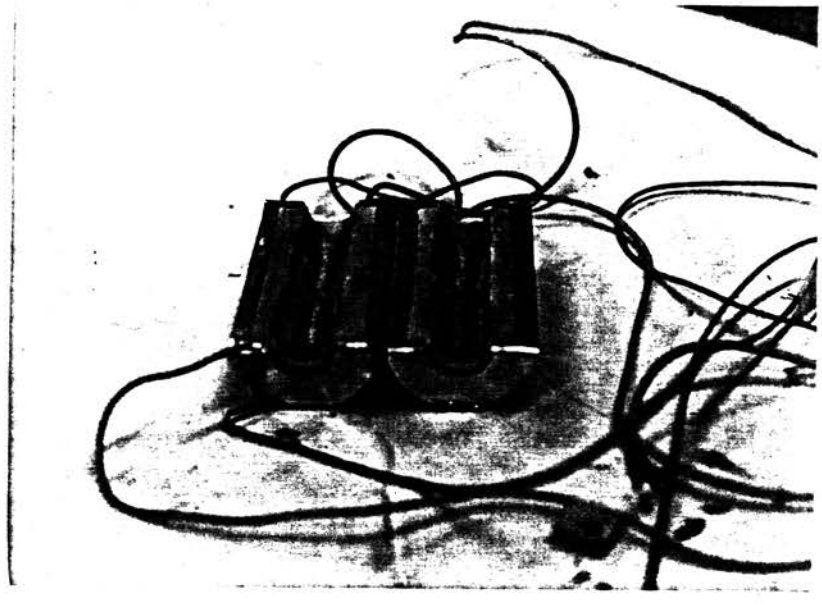

Fig. 4.1 Heater Used in Experiment

A heater may take one of several forms, as long as heat is applied uniformly and the thermal resistance between the heater and the evaporator section is low.eat losses by radiation and convection to the surroundings should be minimized by applying thermal insulation to the outside of the heater. Where orientation may be varied, long leads between the heater and the instruments should be used for convenience.

(ii) Variac for power control

A variac should be incorporated in the heater circuit so that any desired power input may be selected and maintained.

(iii) Voltmeter and Ampmeter for power input measurement

Unit Electric Current-The Ampere. In the MKS system the unit of electric current is defined in terms of force acting on a conductor carrying current and lying in a magnetic field, as follows:

An ampere is that current which, when flowing in each of two parallel straight conductors of infinite length and of negligible cross section, separated by a distance of one meter, in a vacuum, produces on each conductor a force of 2x10 newton per meter of conductor.

Unit Electromotive Force-The Volt. The power in an electric circuit is peopertional to the peoduct of the electromotive force and the current. The ampere having been defined, it is now possible to define the volt in terms of power.

A volt of electromotive force is defined as the instantaneous emf acting in a circuit when, with an instantaneous current of one ampere flowing,the instantaneous power is one watt. It follows therefore that the power in an electric circuit is given by the

equation

$$\text{POWER} = ei \quad \text{watts}$$

where e = volts and i = amperes

In this study, the applied voltage and current are measured separately to obtain the power (watt) input.

(iv) Condenser for heat removal

Dimension of condenser

Inside diameter	7.2	cm.
Outside diameter	7.6	cm.
Length	15	cm.

An effective technique for measureing the rate of heat transfer of a heat pipe operating at vapor temperatures appropriate to most organic fluids and water is to use a condenser jacket through, which a liquid is passed. For many cases this may be water. The heat given up to the water can be obtained if the temperature rise between the condenser inlet and outlet is known, together with the liquid flowrate. The temperature of the liquid flowing to the jacket may be varied to change the heat pipe vapor temperature.

(v) Thermocouples for temperature measurement and associated readout system

The measurement of the temperatures peofiles along the heat pipe is normally carried out using CA type thermocouples (320 micron Ø) attached to the heat pipe outer wall and also to the heater, the condenser and the insulator outer walls. To investigate the transient behavior, for example, during startup , burnout , an automatic electronic data collection is necessary. For steady state operation,

a switching box connected to a digital voltmeter or a multi-channel recorder should suffice.

(vi) Provision for tilting heat pipe

provision has been made on the rig to rotate the heat pipe through 180 while keeping heater and condenser in operation. The angle of the pipe can be set and measured.

(vii) Thermal insulation

As a protection against radiation heat input, the heat pipe, fluid lines and cold wall should all be covered with insulation. The dimension of fiber-glass insulation used in this experiment is shown in TABLE 4.1

TABLE 4.1 Dimension of Insulation Used in The Experiment

	Heating section	Adiabatic section	Cooling section
ID (cm)	7.2	0.8	7.6
OD (cm)	17.2	17.2	17.6

(viii) Provision for measuring flowrate and temperature rise of condenser coolant

The flowrate is measured by collecting and measuring the volume of water passing through the condenser in an interval of time, for example, 100 cm^3/1 minute.

The temperature rise of the condenser coolant is measured by using a thermopile attached to the entrance and the exit of the condenser. When water from the reservoir flows to the condenser, the thermopile will register the inlet-outlet temperature difference and

turns into voltage signal, which is then displayed by a millivolt meter.

4.2 Experimental Procedure

Once the heat pipe is fully instrumented and set up in the rig, the follcwing peocedures are

1. Set the heat pipe at a number of angles to the horizontal. At first keep the heat pipe to the horizontal ($\Psi = 0$)

2. Control the volume flowrate of water in / water out at an appropriate and steady value during the experimental run.

3. Apply power input to the evaporator at time $t = 0$

4. record data of temperature profile along the heat pipe and insulators. Also note down the water flow rate and inlet-outlet temperatures at regular time intervals until the temperture profiles reachs some steady state.

5. To carry out another run for a different power input, shut down the system and wait until everything returns to normal. Then repeat step 2 and 3.

6. Repeat step 5 until having enough data for a particular angle of inclination. Repeat step 2 to 5 until enough angles have been studied.

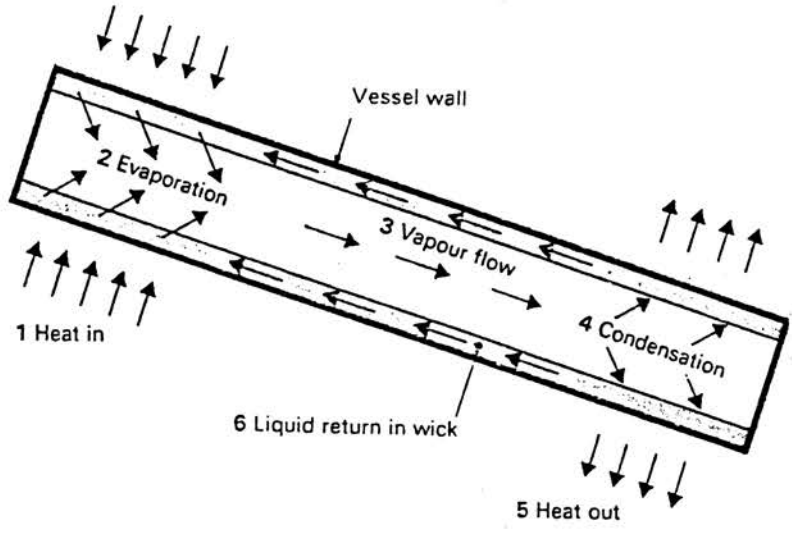

Fig. 4.2 Heat pipe operation

4.3 Experimental Conditions Investigated

In order to study the dynamic behavior of the heat pipe in this experiment, we are interested in the time response of temperature at a number of points along the heat pipe and the instantaneous heat flux through the heat pipe. At an angle of interest, each test was carried out by applying a different heat input rate to the heat pipe which was initially at room conditions. Four different heat inputs were used at each angle and three different angles of inclination of the heat pipe with respect to the horizontal ($0 \leq \Psi \leq 90$) operating in the antigravity mode, were investigated.

The experimental conditions are summarized in Table4.2 , and a sketch of the tilted heat pipe is shown in Fig. 4.3

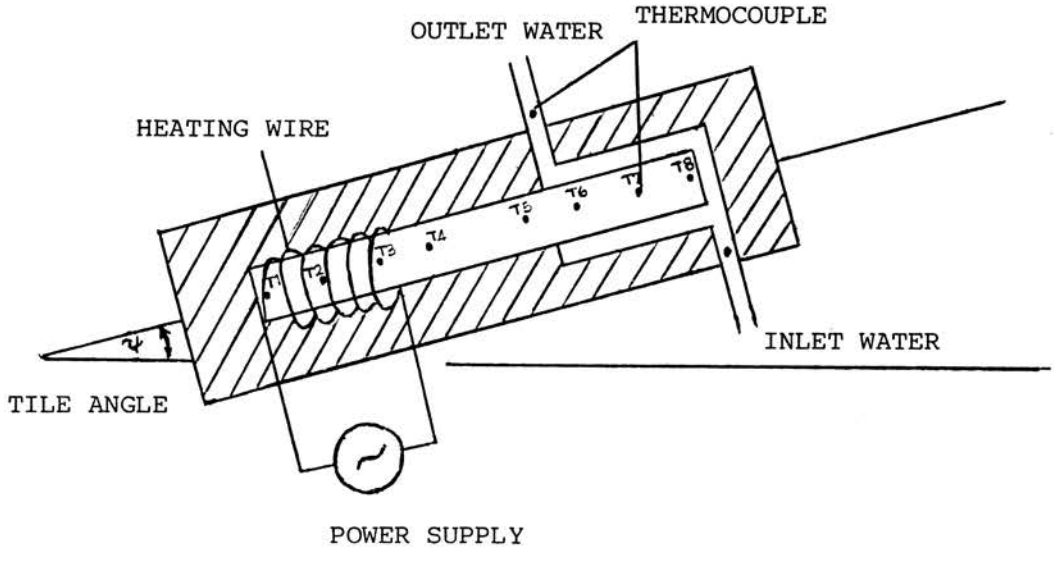

Fig. 4.3 Detail of Heat Pipe Experimentation

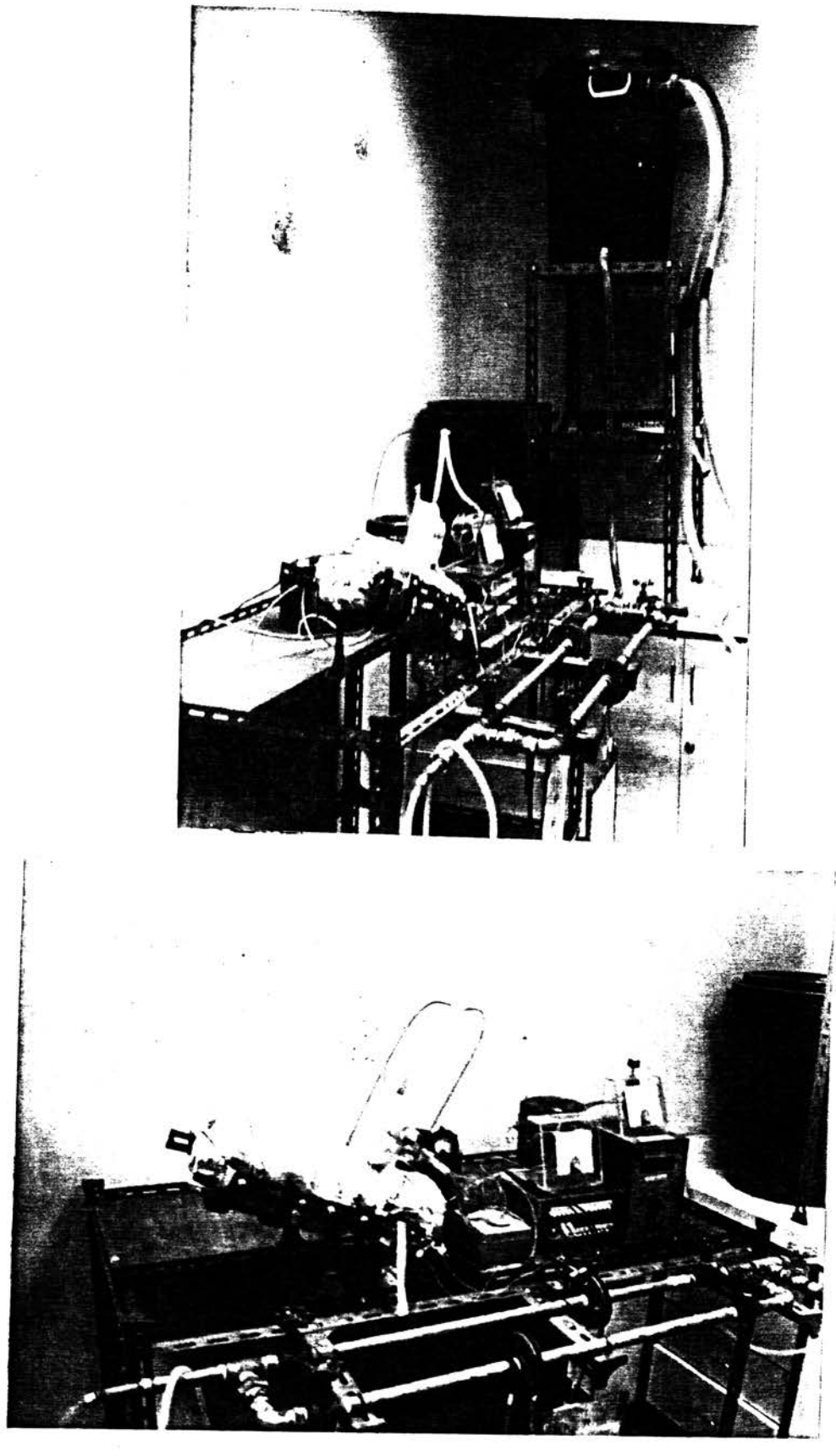

Fig. 4.25 Photagraphs of experimental apparatus

TABLE 4.2 Various tilt angles (antigravity angles measured from horizontal) and heat inputs.

Tilt angle of heat pipe (degree)	Heat input (watt)
10	5.34 7.58 13.08 33.23
20	5.42 7.60 13.06 20.12
30	5.45 7.5 13.12 16.45

4.4 Experimental results

4.4.1 Characteristics of Tested Heat Pipe

A copper heat pipe with water as the working fluid was used in the experiments. The heat pipe has the following characteristics :

Length	300	mm.
Outside diameter	8	mm.
Inside diameter	6.4	mm.
Material of pipe	Copper	
Wick structure	3 layer, (150-mesh screen)	

Wick wire diameter	0.066	mm.
Wick thickness	0.396	mm.
Calculated porosity	0.686	mm.
Wick material	brass	
Working fluid	water	
Working fluid quantity	1.47	gm.
Vapor core diameter	5.6	mm.
Pipe wall thickness	0.8	mm.
Evaporator length, L_e	90	mm.
Adiabatic length, L_a	100	mm.
Condenser length, L_c	110	mm.
Temperature detectors	CA thermocouples (320 μ Ø) 8 pairs	

From the graphs in Figs. 4.5 - 4.16, we see that the time response of the heat pipe surface temperatures appear to be of linear first-order system. By assuming so, we can then determine the time constants of the system under various operating conditions. The results are summarized in Table 4.4.1 . We may then conclude that the time constant of the tested heat pipe is essentially independent of the applied heat input, but depends slightly on the tilt angle. Since the heat pipe is in the top heating mode (antigravity), when the tilt angle increases, the working fluid must try harder, and thus take a little longer, to return to the evaporator section against gravity.

The fact that the dynamic behavior of the heat pipe can be approximated by a first order system is very interesting and useful. It tells us that we may well use a simple empirical model, instead of the present elaborate lumped-parameter transport model, to predict the time response (startup) of the heat pipe, provided the approximate time constant has been found a priori.

We may conclude from Figs 4.17 - 4.21 that the heat transfer rate of the heat pipe generally decreases when the antigravity tilt angle increases with the heat input being kept constant. At the same tilt angle, it is natural that the heat transfer rate increases as heat ixput increases. Regarding the axial temperature profile of the heat pipe , we see that the temperature difference between the heating and cooling sections of the heat pipe is very small and remains essentially constant when the heat input is low (especially below 10 W.) . The difference generally increases when the anti-gravity tilt angle increases while the heat input is kept constant.

According to Figs 4.22 - 4.24 , there appears to be a linear correlation between the heat input to the heating wire and the heat transfer rate through the heat pipe, when the limiting transfer rates are diregarded. The obtained correlation turns out to be $y = ax$, where y is the heat transfer rate (W) , x is the heat input (W), and $a = 0.6$ is the slope. Thus when no limiting mechanisms occurs, this correlation may be used to predict the steady-state heat transfer rate at any tilt angle . The value of a will depend on the particular system, especially the type and thickness of the insulation.

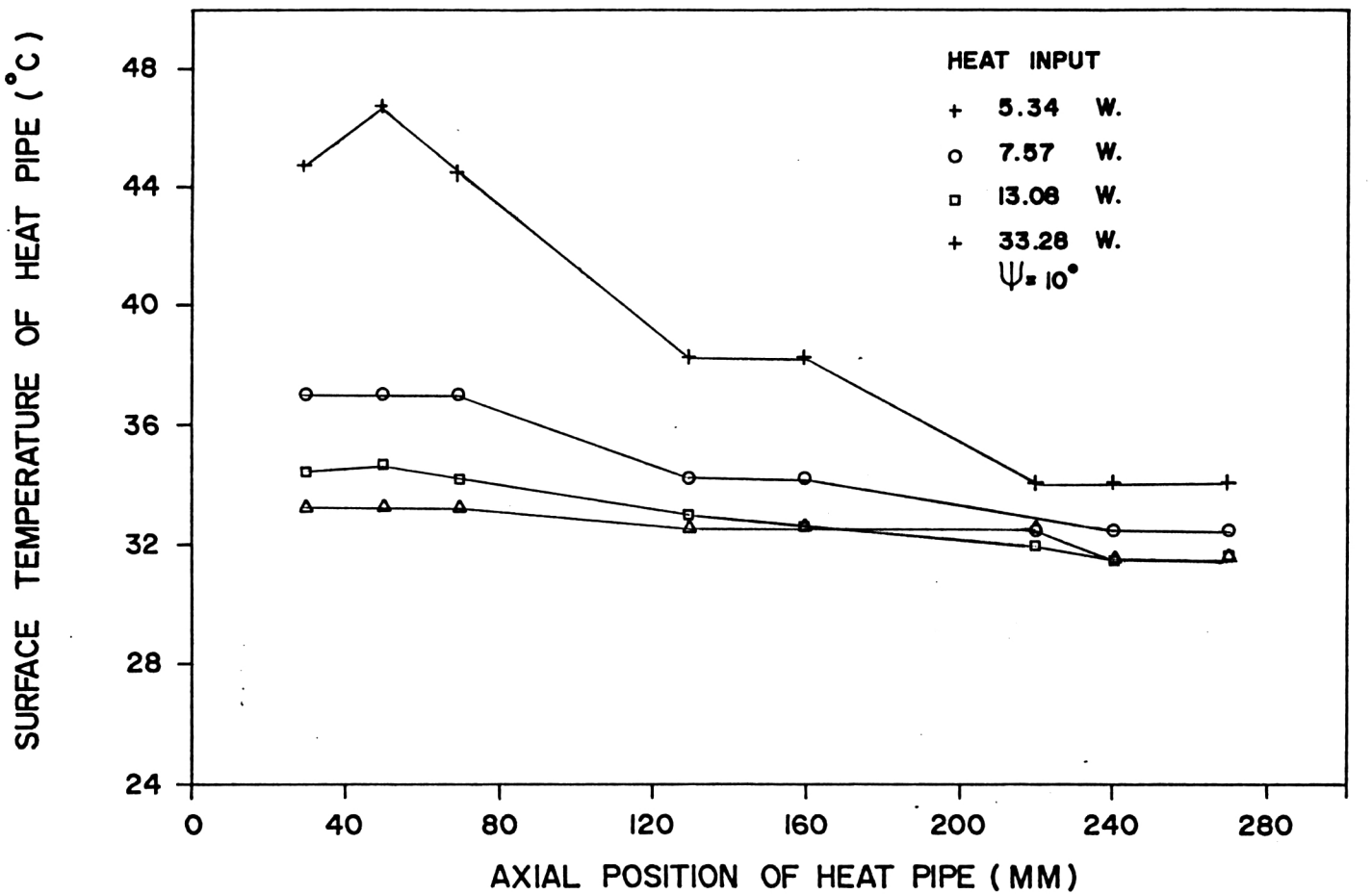

Fig. 4.4 Temperature Profile of Heat Pipe

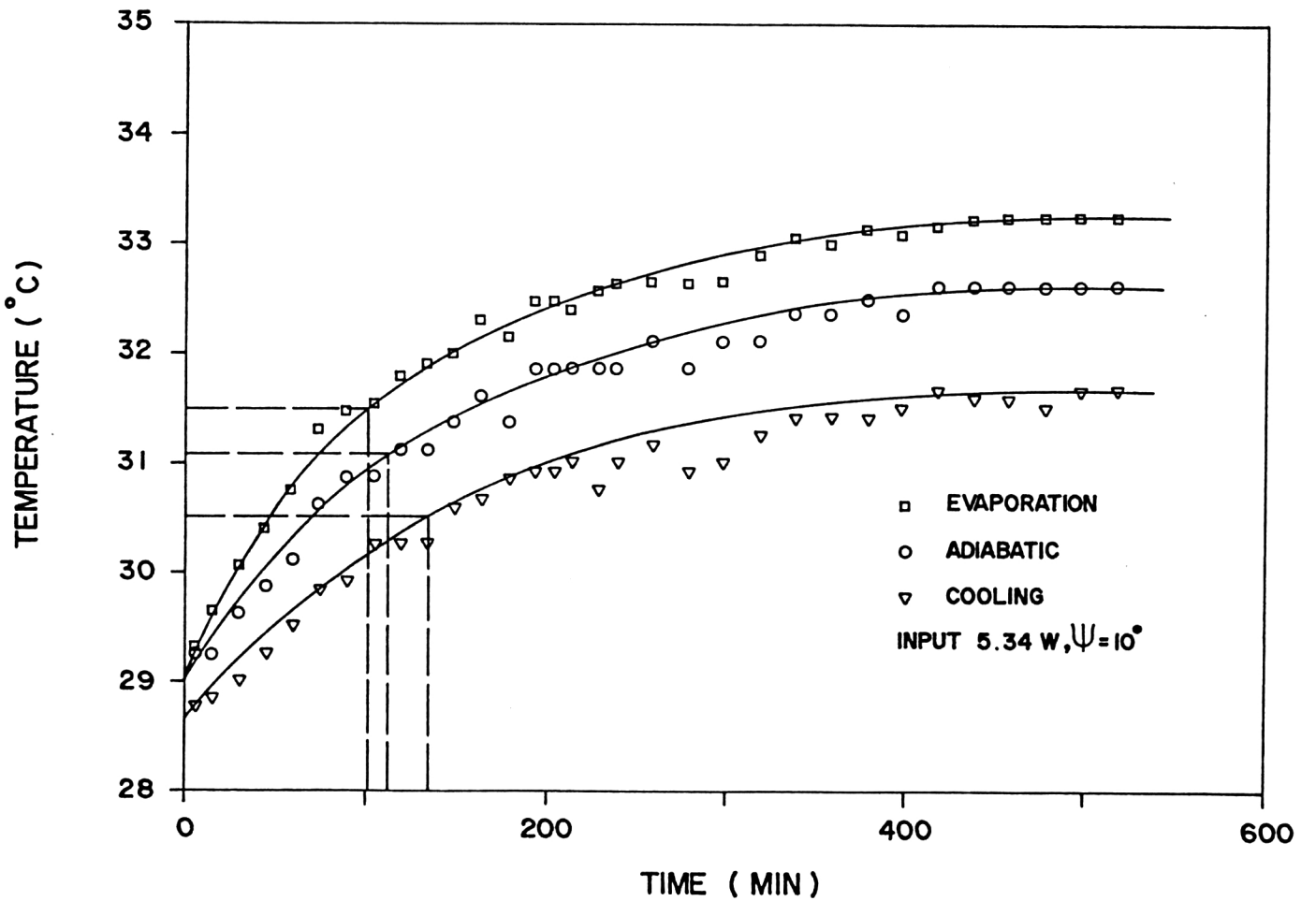

Fig. 4.5 Time Response of Heat Pipe Surface Temperature.

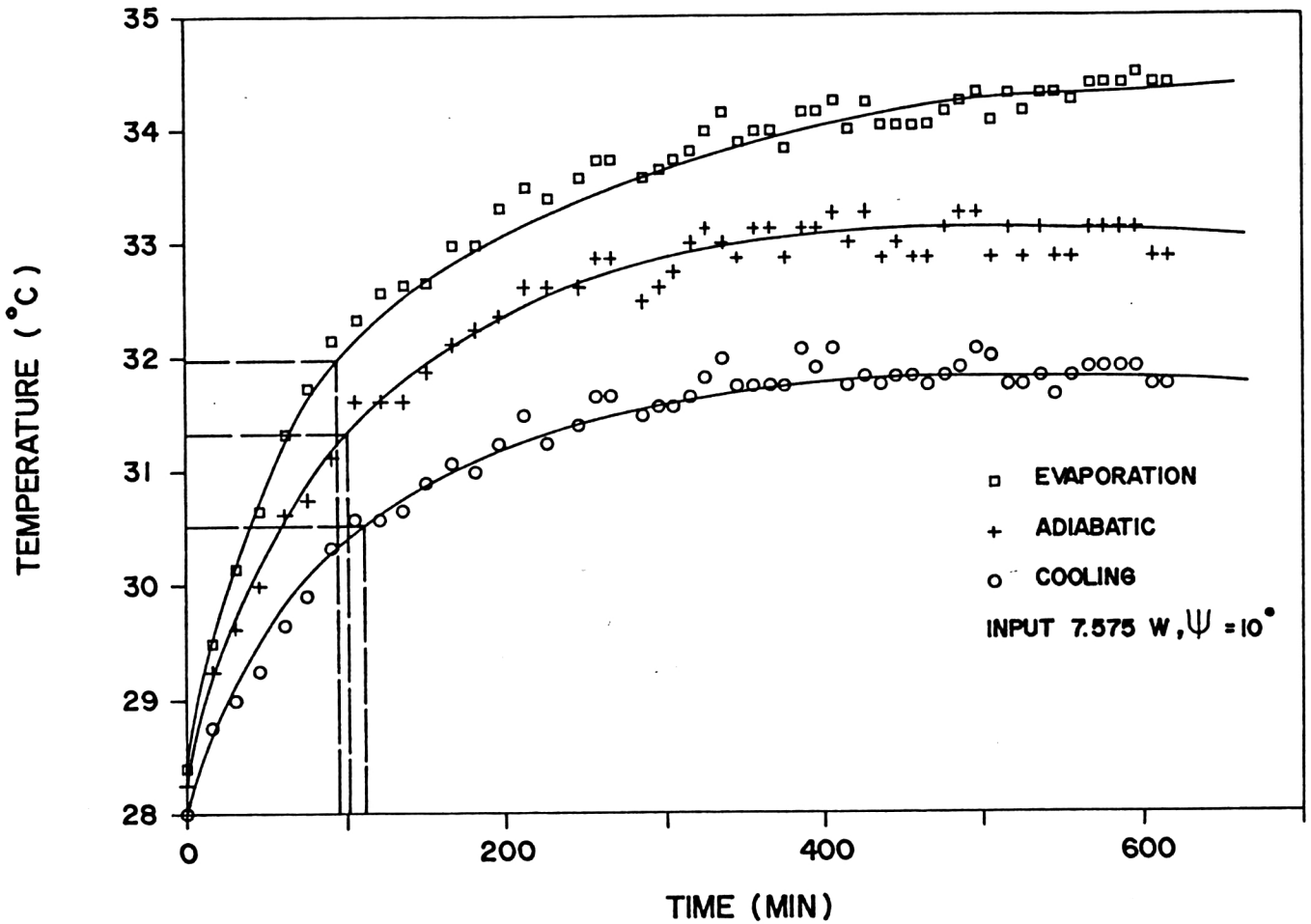

Fig. 4.6 Time Response of Heat Pipe Surface Temperature

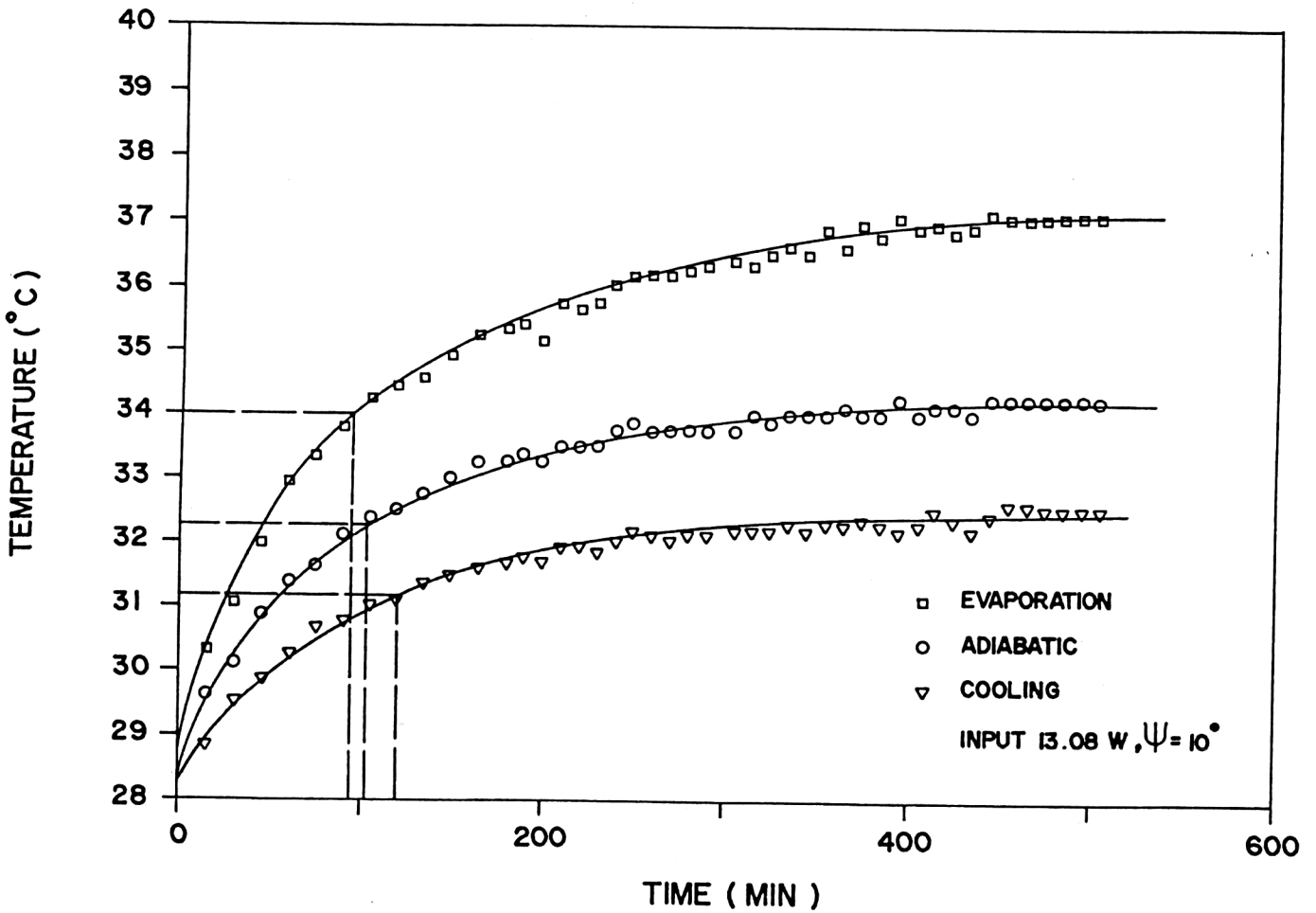

Fig. 4.7 Time Response of Heat Pipe Surface Temperature

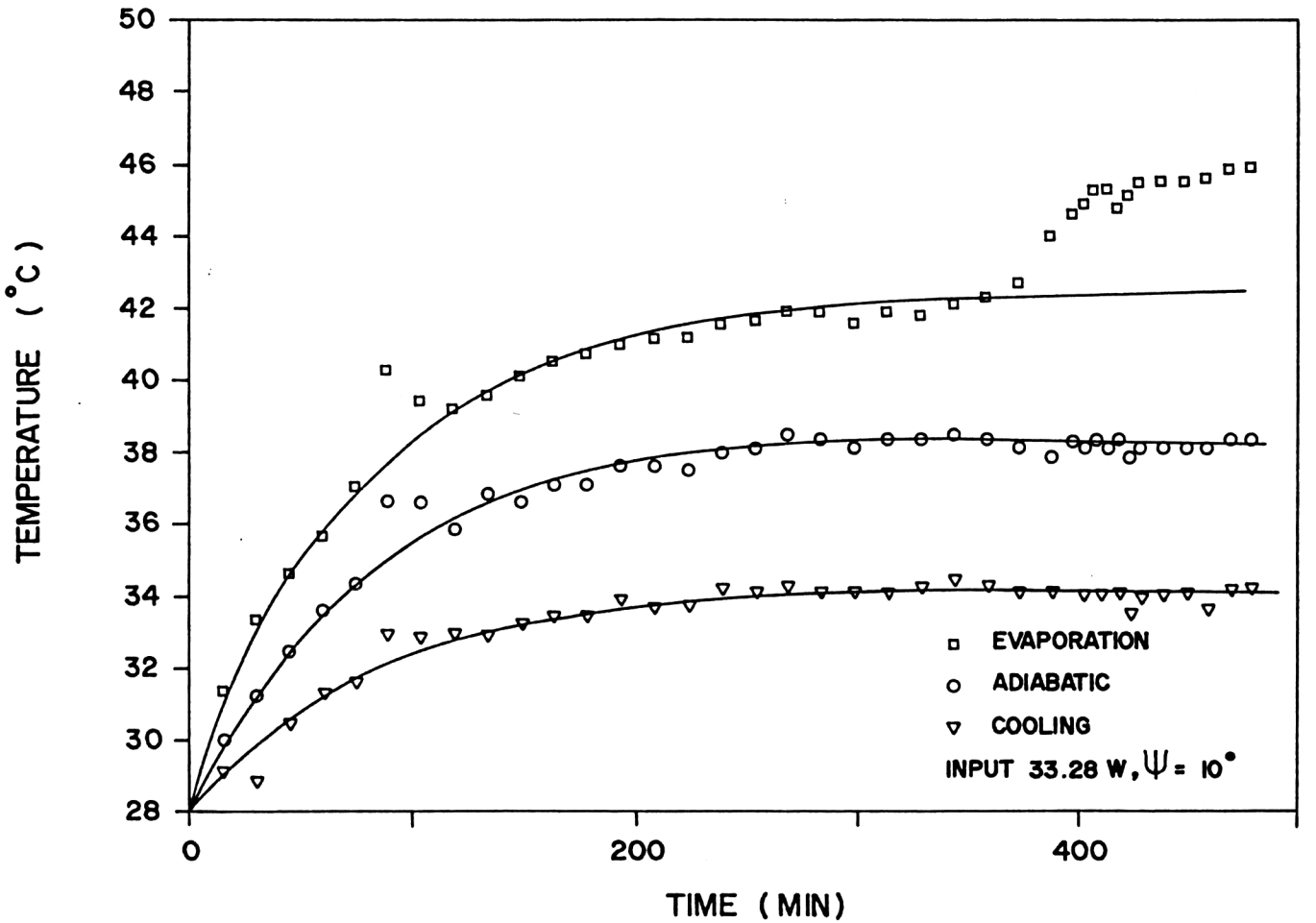

Fig. 4.8 Time Response of Heat Pipe Surface Temperature

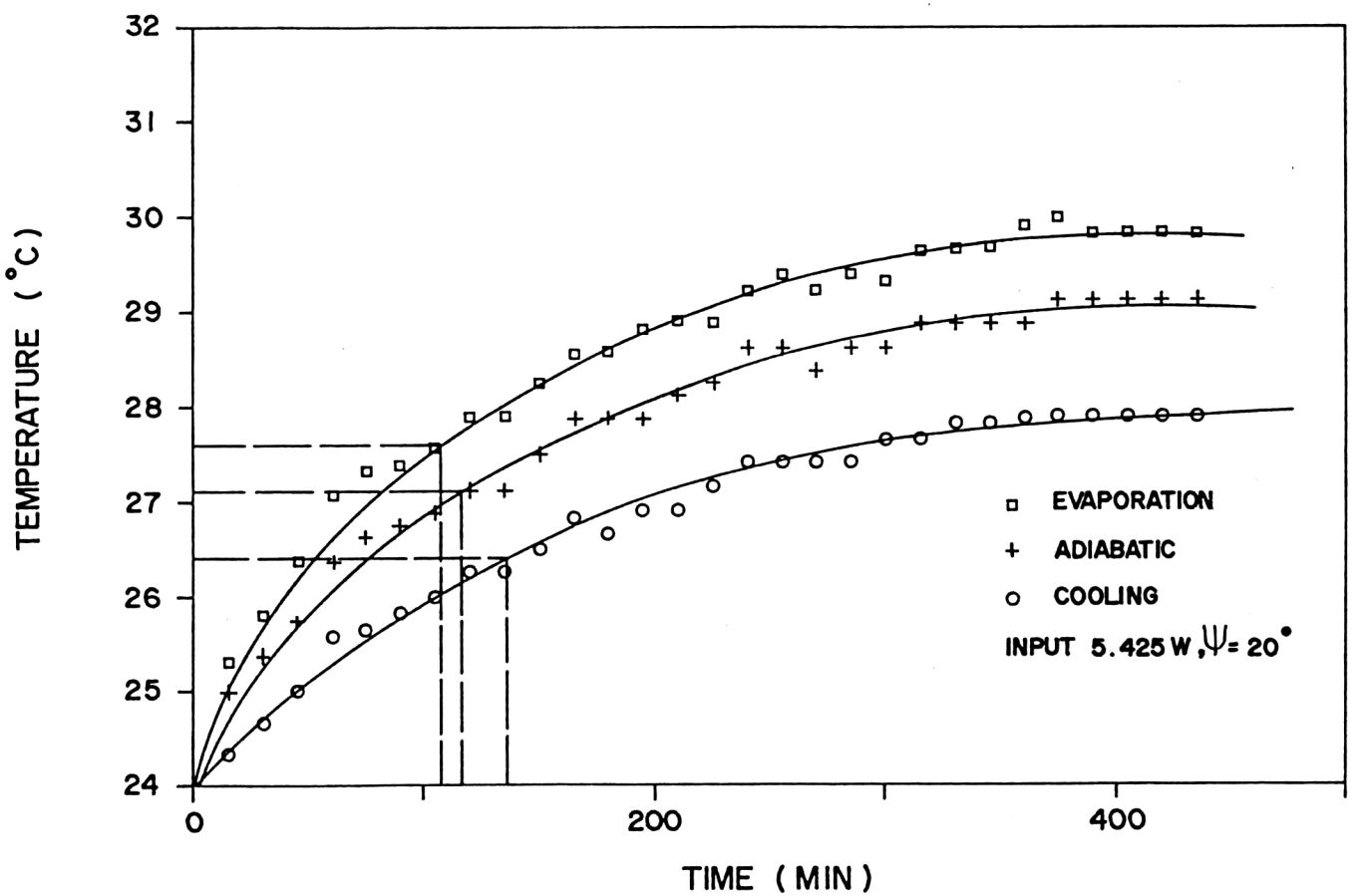

Fig. 4.9 Time Response of Heat Pipe Surface Temperature

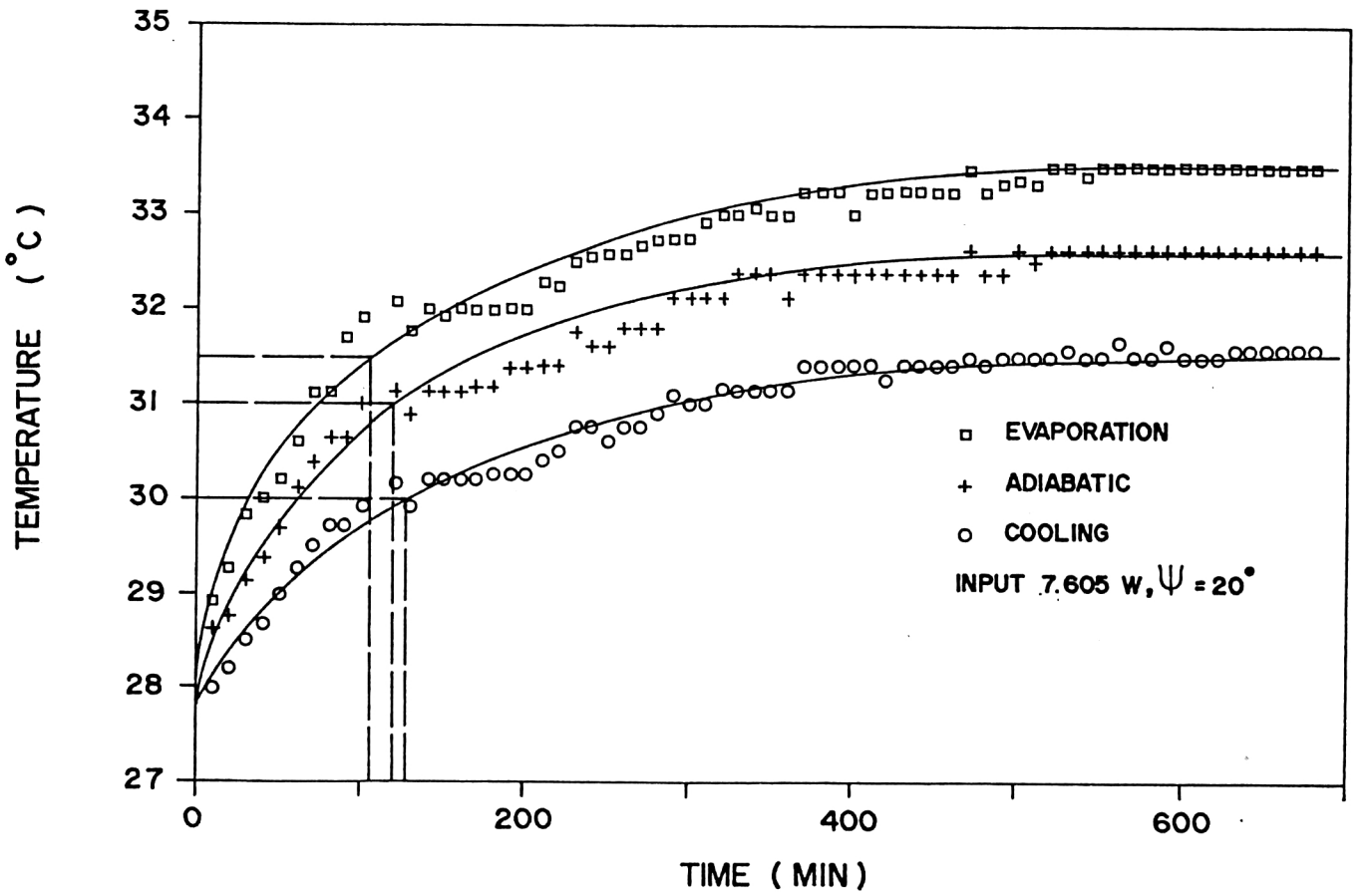

Fig. 4.10 Time Response of Heat Pipe Surface Temperature

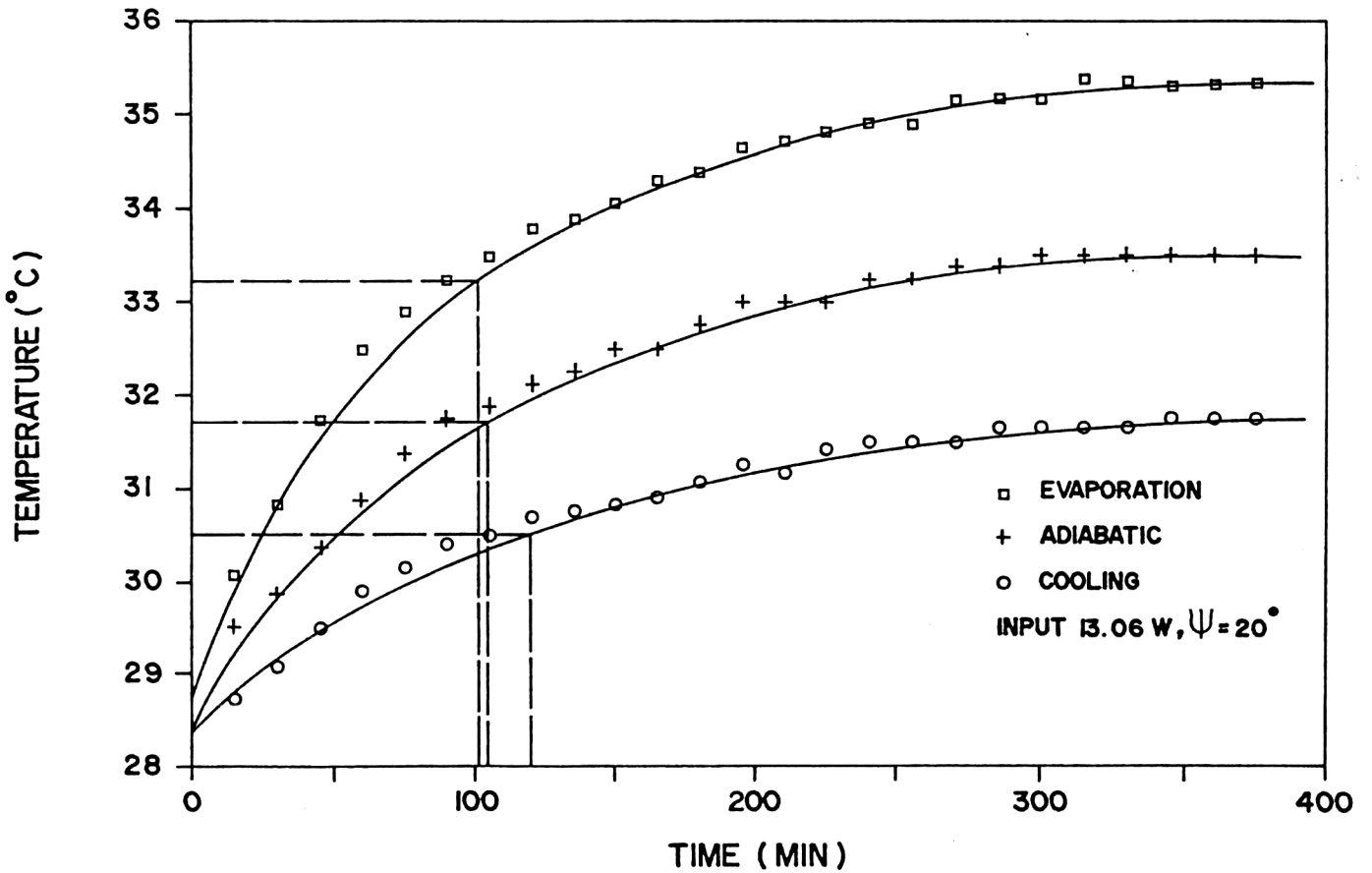

Fig. 4.11 Time Response of Heat Pipe Surface Temperature

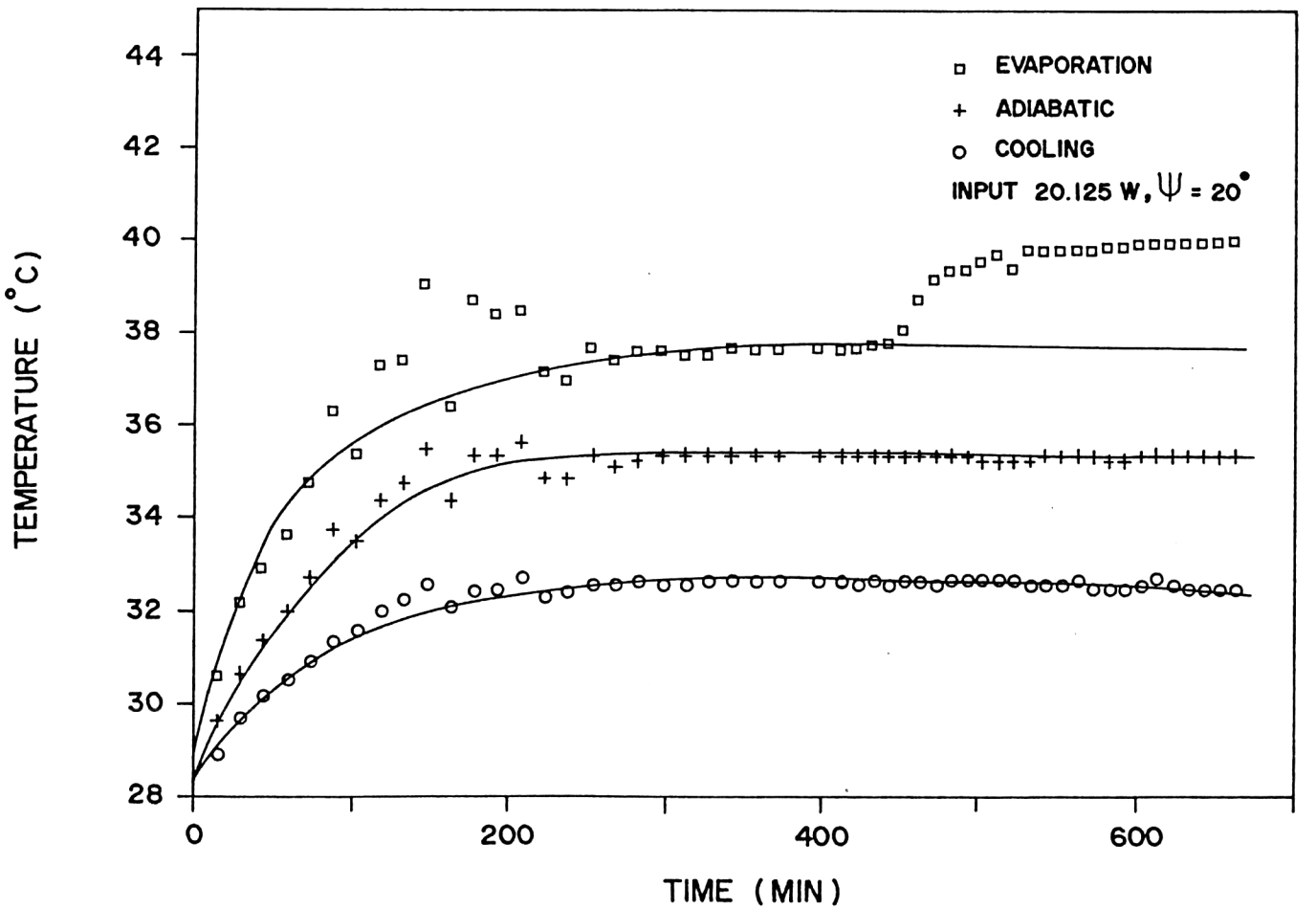

Fig. 4.12 Time Response of Heat Pipe Surface Temperature

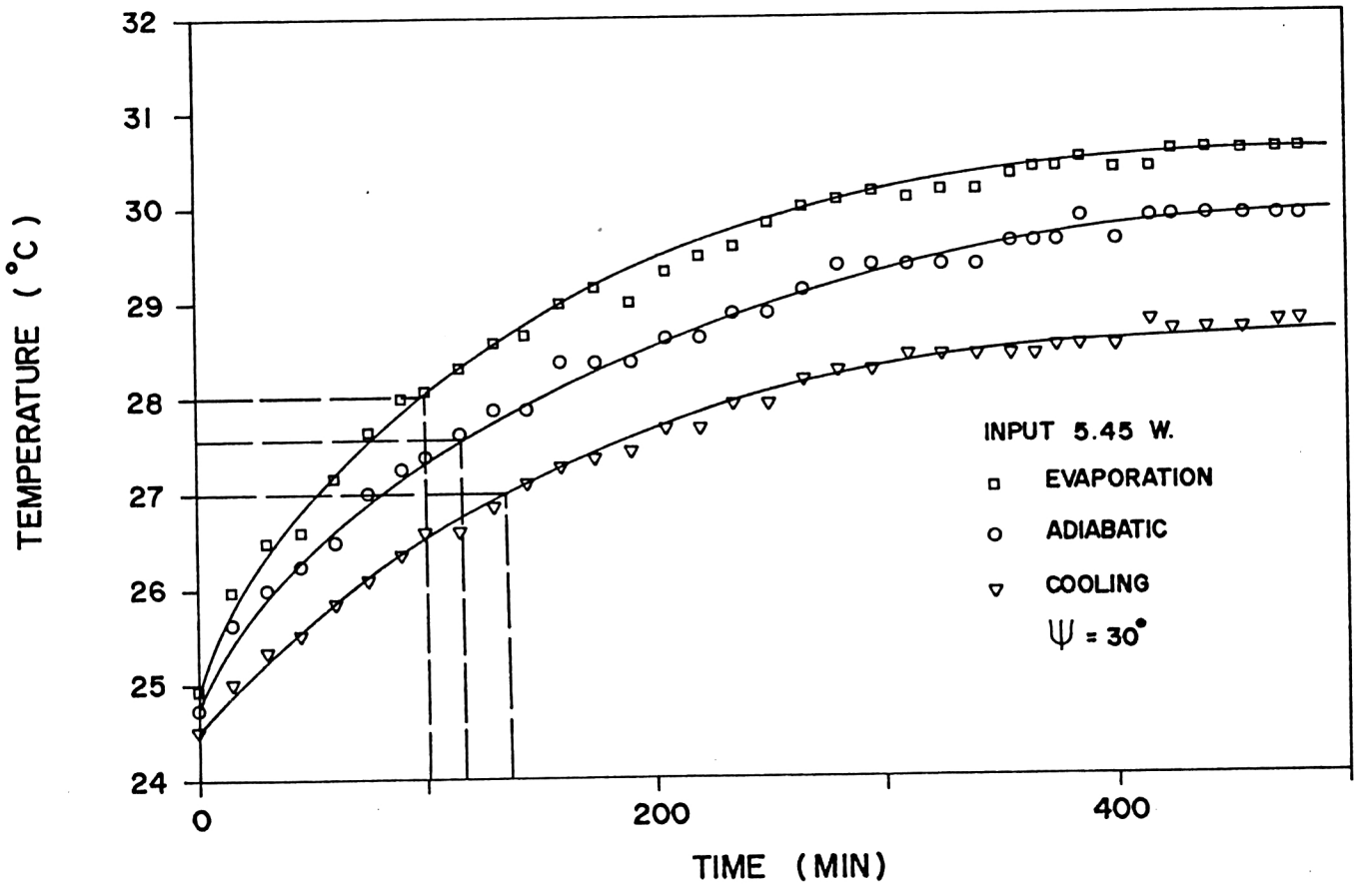

Fig. 4.13 Time Response of Heat Pipe Surface Temperature

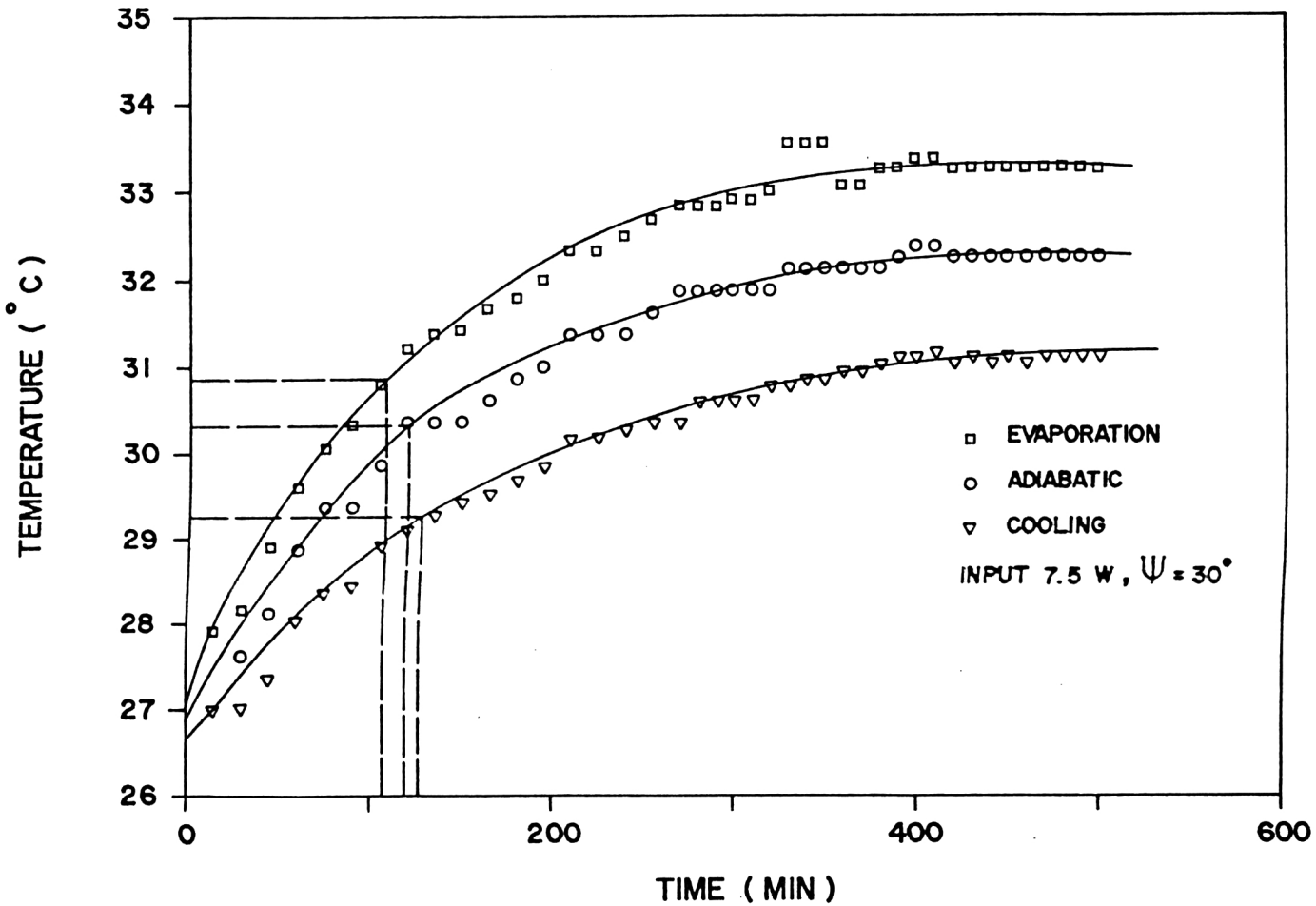

Fig. 4.14 Time Response of Heat Pipe Surface Temperature

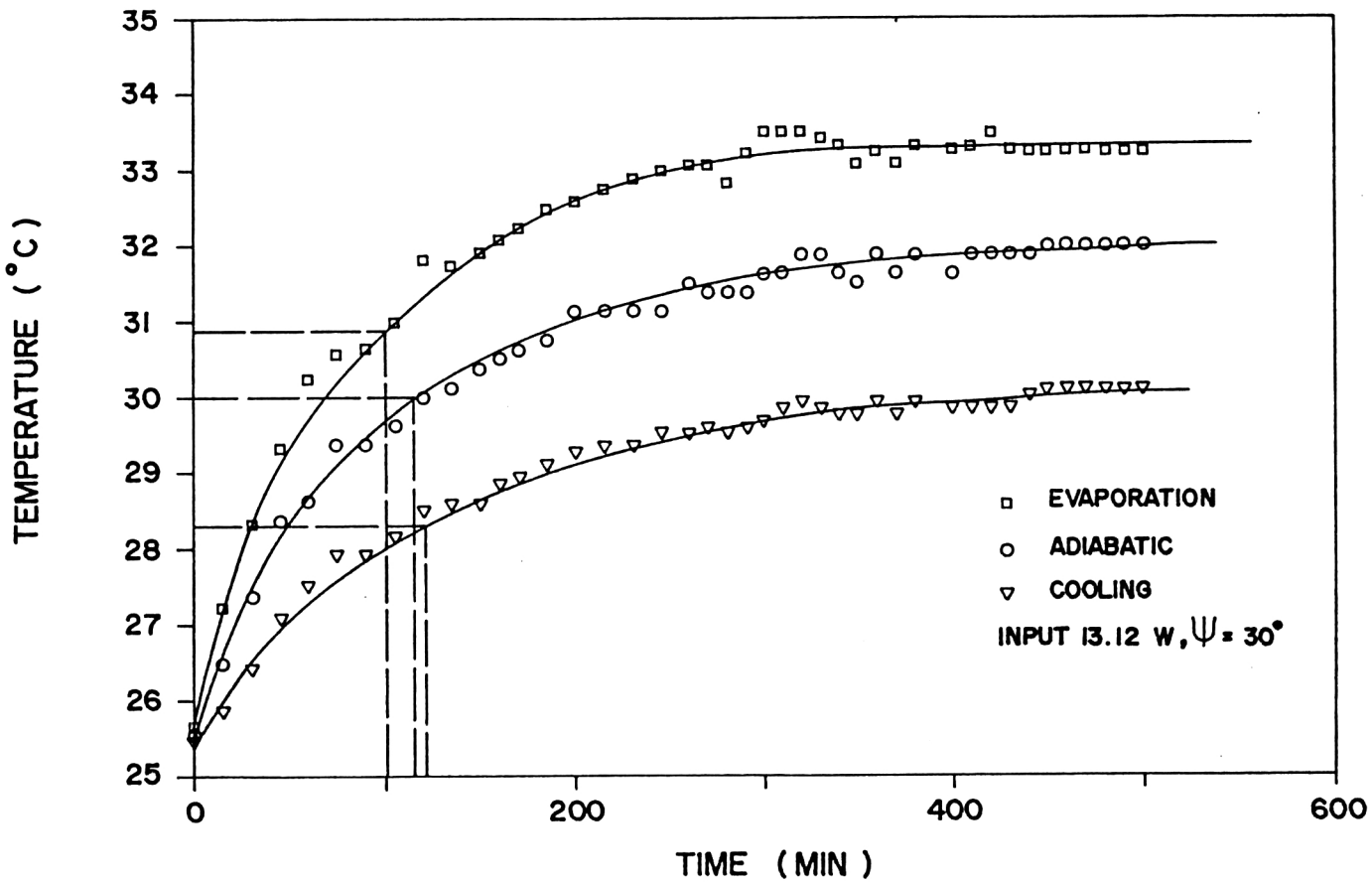

Fig. 4.15 Time Response of Heat Pipe Surface Temperature

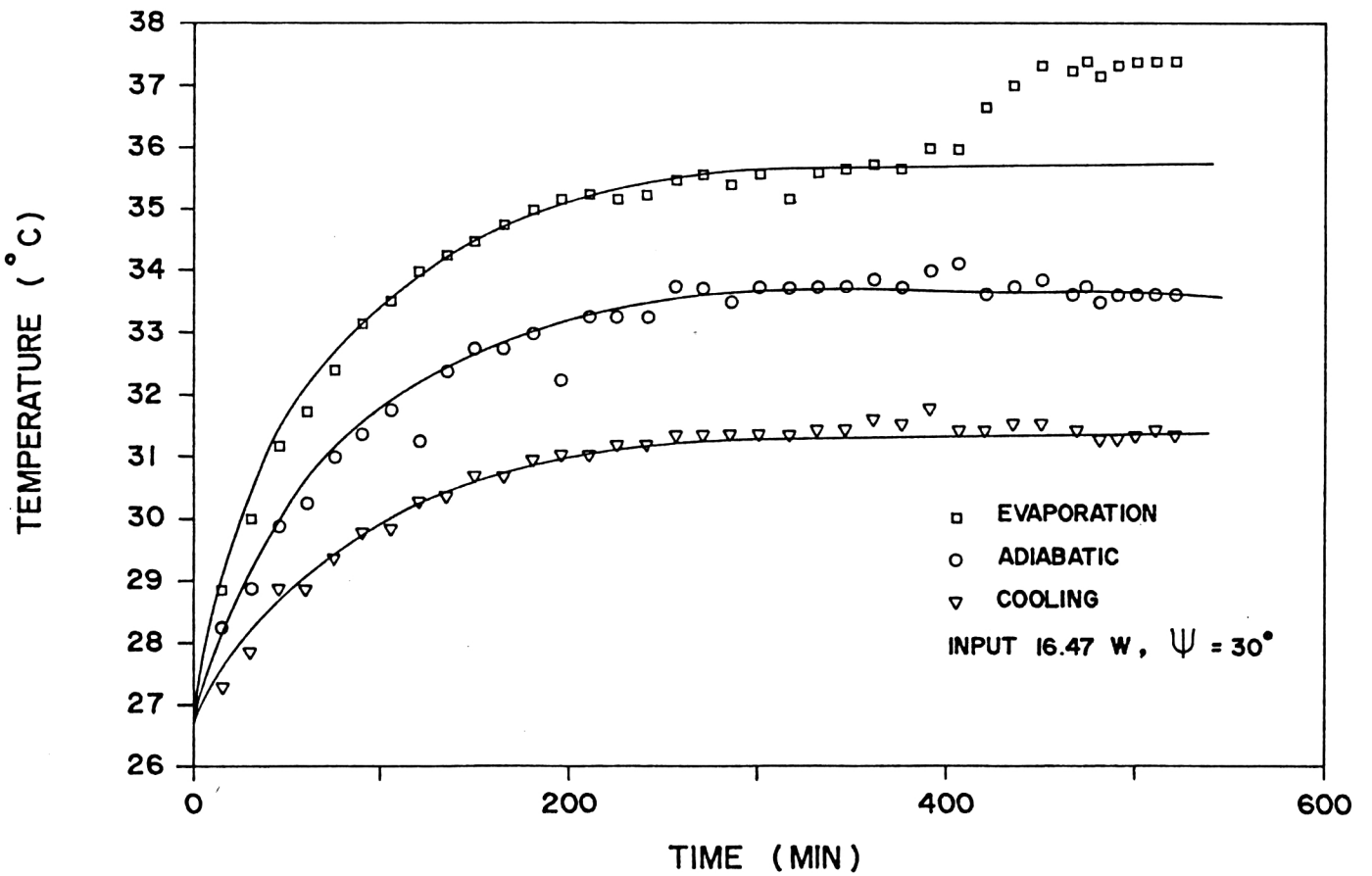

Fig. 4.16 Time Response of Heat Pipe Surface Temperature.

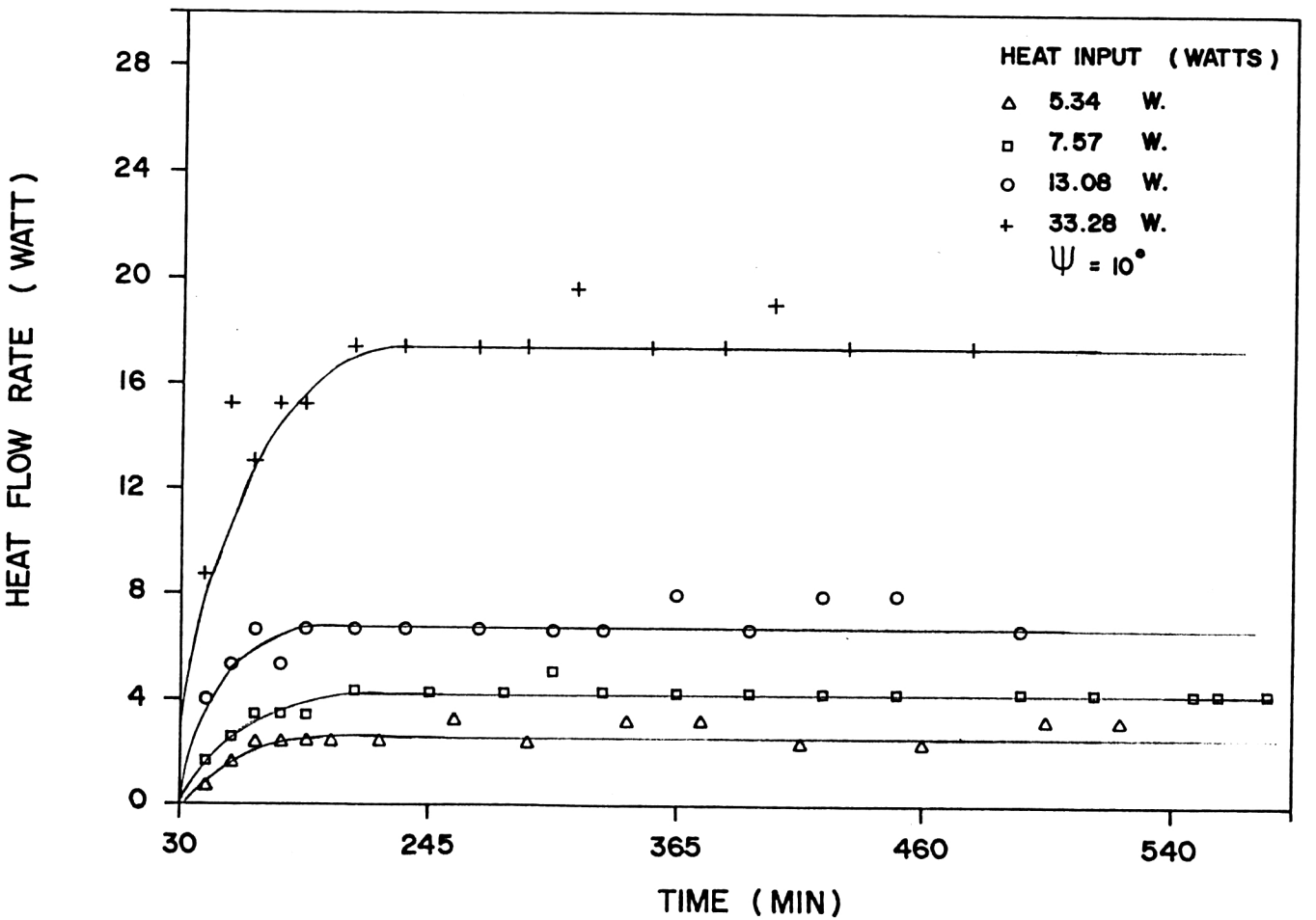

Fig. 4.17 Heat Flow Rate Versus Time

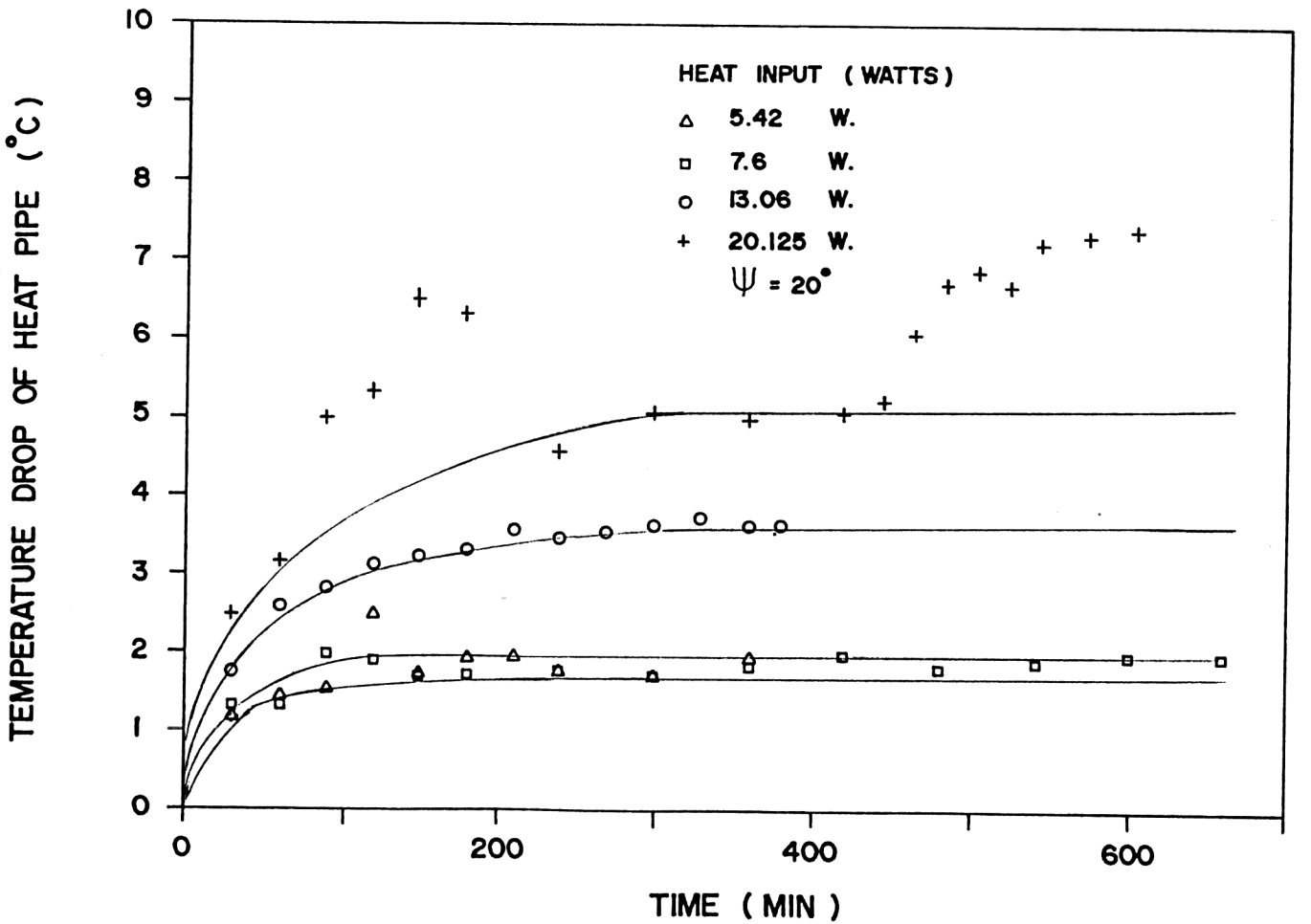

Fig. 4.18 Temperature Drop Versus Time

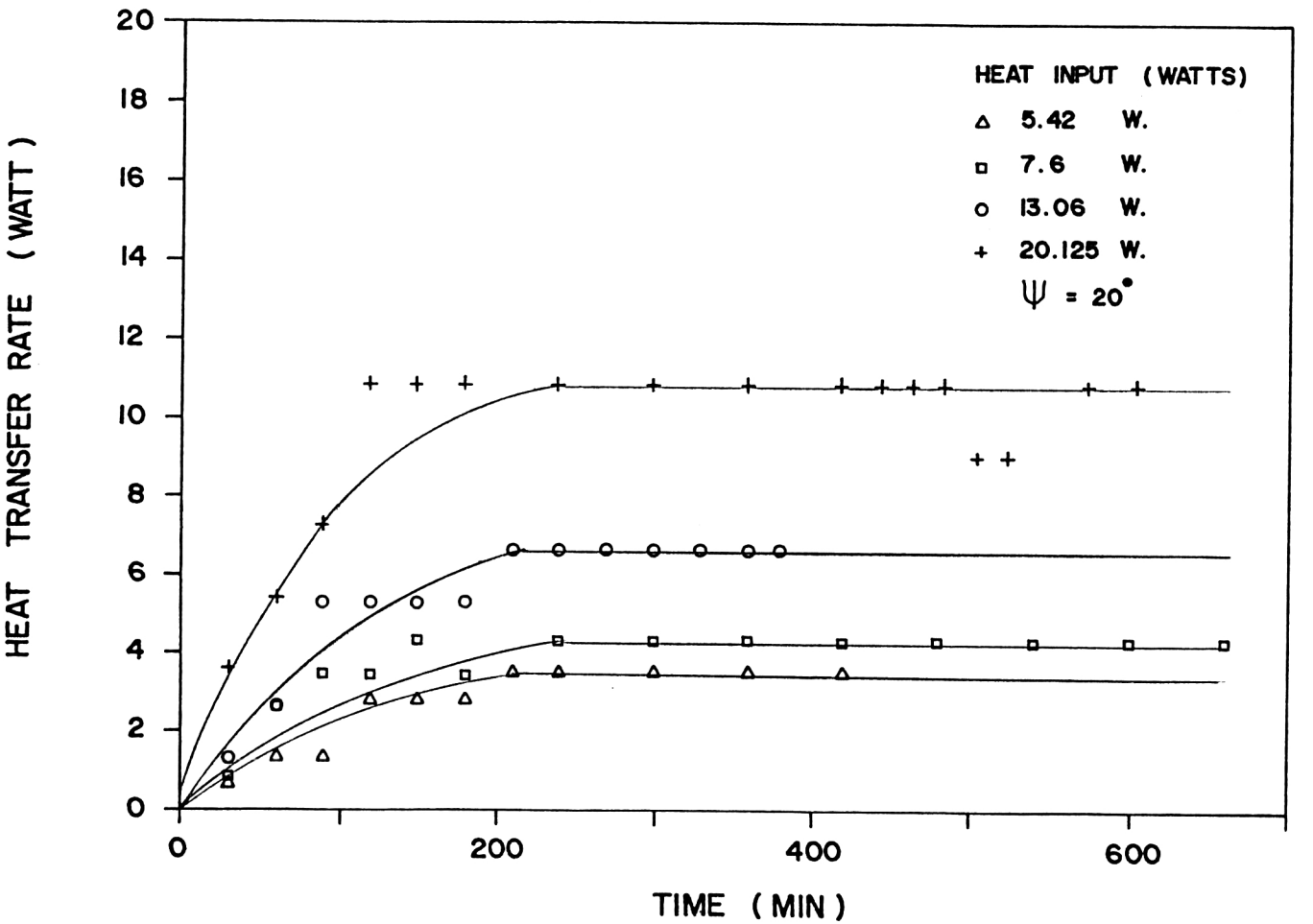

Fig. 4.19 Heat Flow Rate Versus Time

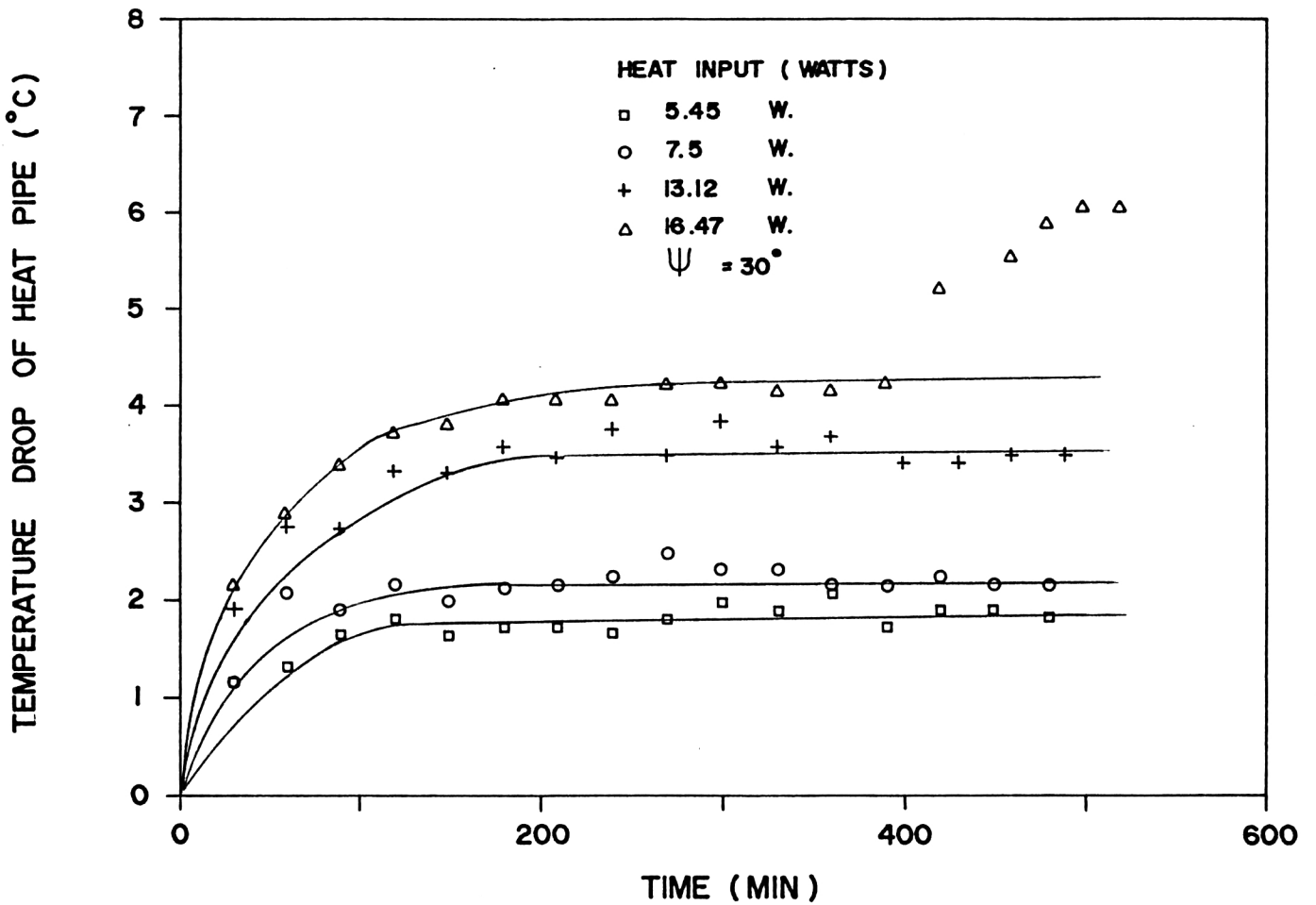

Fig. 20 Temperature Drop Versus Time

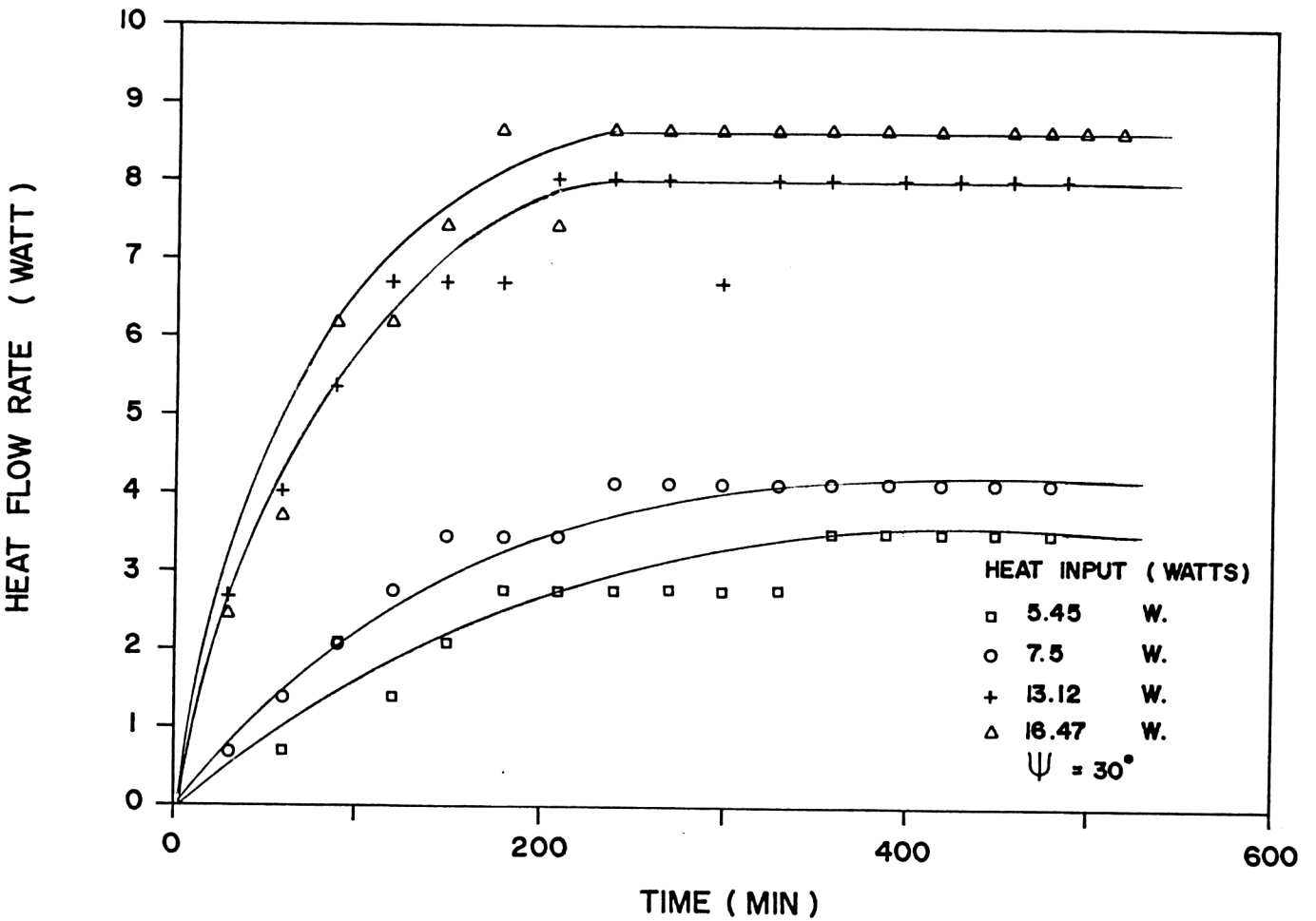

Fig. 4.21 Heat Flow Rate Versus Time

Table 4.3 Time Response to The System at Various Conditions

(based on Fig. 4.5 to Fig. 4.16)

θ (DEGREES)	HEAT INPUT (WATTS)	TIME CONSTANT		
		τ_e evaparation section (MIN.)	τ_a adiabatic section (MIN.)	τ_c cooling section (MIN.)
10	5.34	101	111	129
	7.57	98	109	120
	13.08	96	104	119
	Average	98	108	122
20	5.42	109	116	136
	7.6	103	116	125
	13.06	101	105	121
	Average	104	112	127
30	5.45	103	116	136
	7.5	109	122	129
	13.12	103	111	124
	Average	105	116	129

4.5 Analysis and Discussion of Experimental Results :

4.5.1 Calculation for limit in heat transport capability of the heat pipe

Possible mechanisms limiting heat transport are :

1. Capillary limitation ; $Q_{e,max}$
2. Sonic limitation ; $Q_{s,max}$
3. Entrainment limitation ; $Q_{e,max}$
4. Boiling limitation ; $Q_{b,max}$

The following calculations of varions limiting values made use of experimental data obtained for the case shown in Fig.4.4 , dry-out began to occur at a heat flux of 17.4 watts, apparently because the energy input was a little greater than the ability of the wick to transport condensed liquid from the condensing section back to the evaporation section. This phenomenon caused discontinuity between vapor and liquid flow and effected a sudden increase of temperature at the evaporation section when compared to the other regions of the heat pipe.

Calculation of Limiting Values (For example : The case of tilt angle of 10 degrees, heat input 33.28 watt) From FIG.4.4 ,the dry out temperature of the evaporation section was 44.66 C

Working fluid properties (water) at 44.66 c (Appendix A)			
Latent Heat	(J/kg)		2.391×10^{6}
Liquid Density	(kg/m3		990.1
Vapor Density	(kg/m^3		0.07
Liquid Thermal Conductivity	k_l	(w/m-k)	0.645
Liquid Viscosity		(kg/m-sec)	6.08×10^{-4}
Vapor Viscosity		(kg/m-sec)	1.058×10^{-5}
Liquid surface Tension		(N/m)	6.88×10^{-2}

From Appendix B, the thermal conductivity of the heat pipe and wick materials are as follows :

Thermal Conductivity of Brass	113	W/m· C
Thermal Conductivity of Copper	394	W/m· C

1. Calculation of Capillary Limit

Maximum available pump pressure, P_{pm}

Effective Capillary radius , r_c = 1/2N [m]

Screen mesh number , N = 5.91×10^{-3} [m^{-1}]

Maximum capillary pressure, P_{cm} = $\frac{2\sigma}{r_c}$

= 1626.43 [N/m^2]

Hydrostatic pressure perpendicular to pipe axis, $\Delta P_{\perp}$ = $\rho_l g d_v \cos\Psi$

= 53.56 [N/m^2]

Hydrostatic pressure parallel to pipe axis

$$= \rho_l g L_t \text{SIN}\Psi$$

$$= 505.98 \ [N/m^2]$$

$$P_{pm} = P_{cm} - \Delta P - \rho_l g L_t \text{SIN}\Psi$$

$$= 1066.89 \ [N/m^2]$$

Frictional coefficient for liquid flow, F_l

$$F_l = \mu_l / K A_w \lambda \rho_l$$

Wick Permeability from Table 3.2

$$K = \varepsilon^3 d^2 / 122 (1 - \varepsilon)^2$$

$$= 1.07 \times 10^{-10} \ [m^2]$$

Wick cross-sectional area, A_w

$$= \frac{\pi}{4} (d_i^2 - d_v^2)$$

$$= 7.54 \times 10^{-6} \ [m^2]$$

$$F_l = \frac{6.08 \times 10^{-4}}{(1.07 \times 10^{-10})(7.54 \times 10^{-6})(990.1)(2.39 \times 10^6)}$$

$$= 318.34 \ [(N/m^2)/(W\text{-}m)]$$

Frictional coefficient for vapor flow, F_v

Hydraulic radius for vapor flow, $r_{h,v} = d_v/2 = 2.8 \times 10^{-3}$ [m]

Vapor core cross-sectional area, $A_v = \frac{\pi}{4} d_v^2 = 2.46 \times 10^{-5}$ [m^2]

$$(f_v Re_v) = 16$$

$$F_v = \frac{(f_v R_{ev})\ \mu_v}{2A_v r_{h,v}^2 \rho_v \lambda}$$

$$= 2.62\ [(N/m^2)/(w\text{-}m)]$$

Capillary limit on heat transfer rate, $Q_{c,\,max}$

$$= \frac{(QL)_{c,max}}{\frac{1}{2} L_c + L_a + \frac{1}{2} L_e}$$

$$(QL)_{c,max} = \frac{P_{pm}}{F_l + F_v}$$

$$= 3.324\ [W\text{-}m]$$

$$Q = 17.05\ [W]$$

2. Calculation of Sonic Limit

Vapor specific heat ratio, $\gamma_v = 4/3 = 1.33$

Universal gas constant, $\bar{R} = 8.314 \times 10^3$ [J/kg-mol K]

Gas Molecular Weight, $M = 18$

Gas Constant for vapor, $R_v = \bar{R}/M = 461.89$ [J/kg.K]

Vapor Temperature, $T_v = 417.82$ [K]

$$Q_{s,\,max} = A_v \rho_v \lambda \left[\frac{\gamma_v R_v T_v}{2(\gamma_v + 1)}\right]^{\frac{1}{2}}$$

$$= 843 \quad [W]$$

3. Calculation entrainment Limit

Hydraulic radius of wick at vapor-wick interface,

$$r_{n,s} = \frac{1}{2N} - \frac{d}{2} = 5.16 \times 10^{-5} \quad [m]$$

$$Q_{e,max} = A_v \lambda \left[\frac{\sigma \rho_v}{2\, r_{h,s}}\right]^{\frac{1}{2}}$$

$$= 402 \quad [W]$$

4. Calculation of Boiling Limit

Effective thermal conductivity of liquid-saturated wick, k

$$k_e = \frac{k_l (k_l + k_w) - (1-\varepsilon)(k_l - k_w)}{(k_l + k_w) + (1-\varepsilon)(k_l - k_w)}$$

$$= 1.41 \quad [W/m\text{-}K]$$

Boiling nucleation radius, $r_n = 2.54 \times 10^{-7}$ [m]

Critical pressure $\frac{2\sigma}{r_n} = 5.43 \times 10^{-5}$ [N/m^2]

$$Q_{b,max} = \frac{2 L_e k_e T_v}{\lambda \rho_v \ln(r_i/r_v)} \left(\frac{2\sigma}{rn} - P_c \right)$$

$$= \frac{2\P L_e k_e T_v}{\lambda \rho_v Ln(r_i/r_v)} \left(\frac{2\sigma}{r_n}\right)$$

$$= \frac{2\P(0.09)(1.41)(317.89)(5.43 \times 10^5)}{(2.391 \times 10^6)(0.07)(\ln 3.2/2.8)}$$

$$= 6158 \quad [W]$$

It might be concluded that the various limitting values of heat transport for the heat pipe at working temperature 44.66^{o}C and tilt angle Ψ = 10 degrees (evaporation section is above cooling section) are :

Capillary Limit	17.05	W
Sonic Limit	843	W
Entrainment Limit	402	W
Boiling Limit	6158	W

4.5.2 The heat transport of the tested heat pipe at tilt angle 10 degrees (antigravity namely, evaporation section is higher than the cooling section) for capillary limitation equals 17.046 W, compared to calculated value of 17.4 W. The comparison of the calculated result and experimental result for the case of working temperature 44.66°C; tilt angle 10 degrees thus gives a difference of about ± 3% So we can conclude that capillary limitation limits the heat transport capability of the heat pipe.

4.5.3 One outstanding feature of the heat pipe is the relatively small driving force (temperature difference between the condensation and evaporation sections) required to effect a high heat transfer rate. For example, the experimental result at heat input 7.6 W shows that the heat transfer through the heat pipe is 4.36 W when the temperature difference is only 1-2°C

4.5.4 The underlying physical principle is the transport of heat under a driving temperature difference. There are various proposals to represent the interrelation between heat flow rate and temperature difference with the aid of some characteristic property. Following the suggestions of E.Schmidt (1960) an effective thermal conductivity λ_{eff} is defined here as

$$\lambda_{eff} = LQ/(A_{cross} \Delta T)$$

Where

λ_{eff} = Effective thermal conductivity (W/m-K)

Q = Heat transfer rate of heat pipe (W)

L = Effective length (from the middle of the heating zone to the middle of the cooling zone) (m)

A_{cross} = Cross section area of heat pipe ($A_{cross} = d_i^2 \pi /4$) (m^2)

= Temperature difference between evaporation and condensation sections (K)

Fig. 4.25 is the obtained effective thermal conductivity is shown as a function of time for various heat inputs. We see that at low heat inputs (up to 10 W) the effective thermal conductivity is nearly constant. At higher heat inputs λ_{eff} slowly decreases. The highest observed value is approximatily λ_{eff} 13×10^3 W/m-K, which in comparison with the thermal conductivity of copper ($\lambda_{Cu} \approx 372$ W/m-K) is about 35 times better than a copper rod with the same dimensions as the heat pipe, at the heat transfer rate 4.36 w and tilt angle 20 degrees (antigravity)

In general the effective thermal conductivity will decrease when the angle of heat pipe with respect to horizontal (antgravity) is increased at constant heat transfer rate .

Hahne (Hahne, 1982) tested the performance of a copper thermosyphon (wickless heat pipe) at various tilt angles (gravity assisted) . He found the maximum effective heat conductivity to

be about 85 x 10^3 w/m-K at a tilt angle 40 degrees from the vertical (heat transfer rate2900 W) which was 230 times better than a copper rod. The reason why Hahne's was much more than in this experiment because Hahne's copper thermosyphon was tested in a gravity - assisted condition

4.5.5 Heat transfer rate of the heat pipe decreases when tilt angles increases at a constant heat input . At the same tilt angle, heat transfer rate will increase when heat input increases

4.5.6 Temperature difference between heating and cooling section of the heat pipe is nearly constant at low heat input (especially less than 10 W). The difference will increase when tilt angle of heat pipe increases at constant heat input.

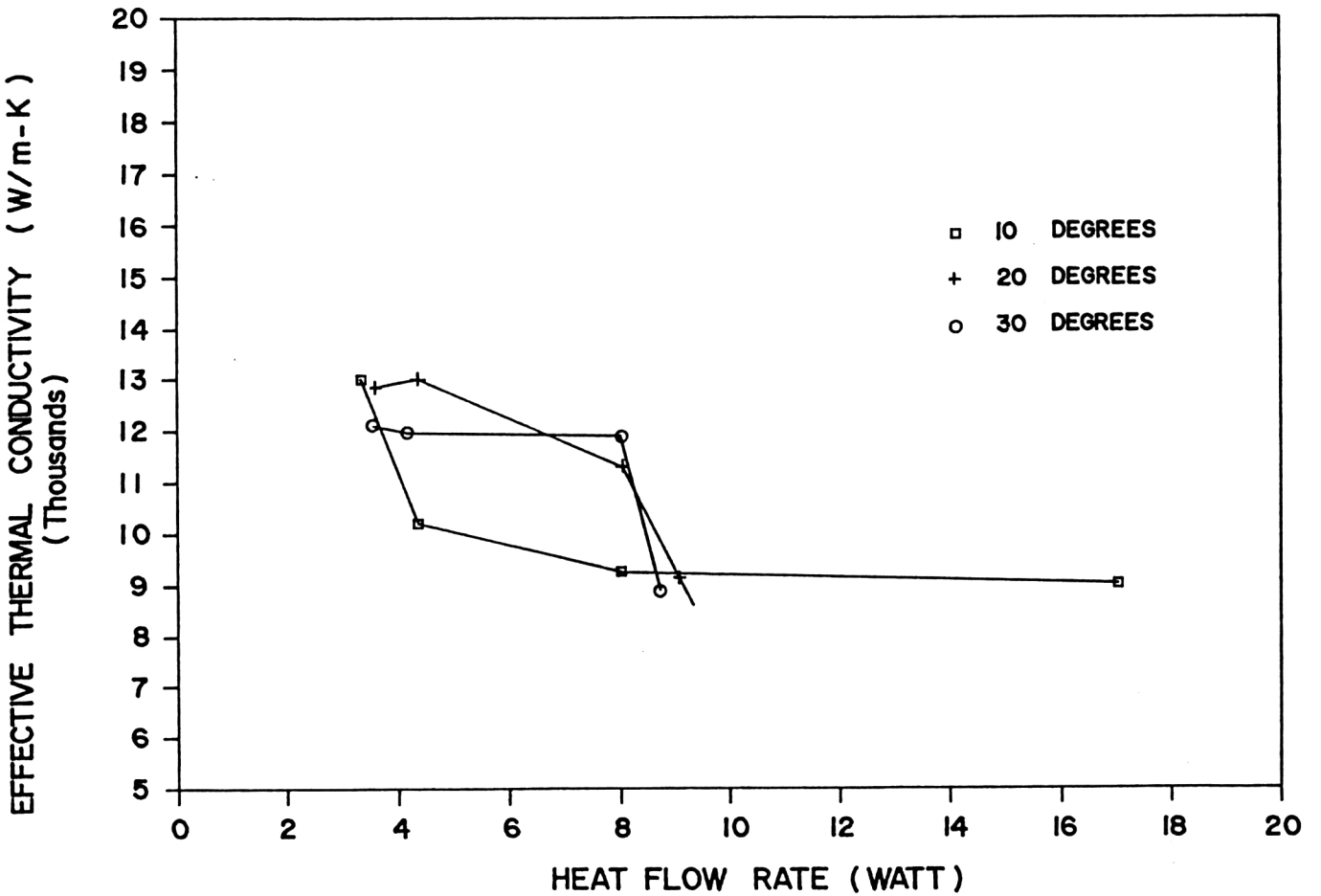

Fig. 4.25 Effect of Heat Flow Rate to Effective Thermal Conductivity

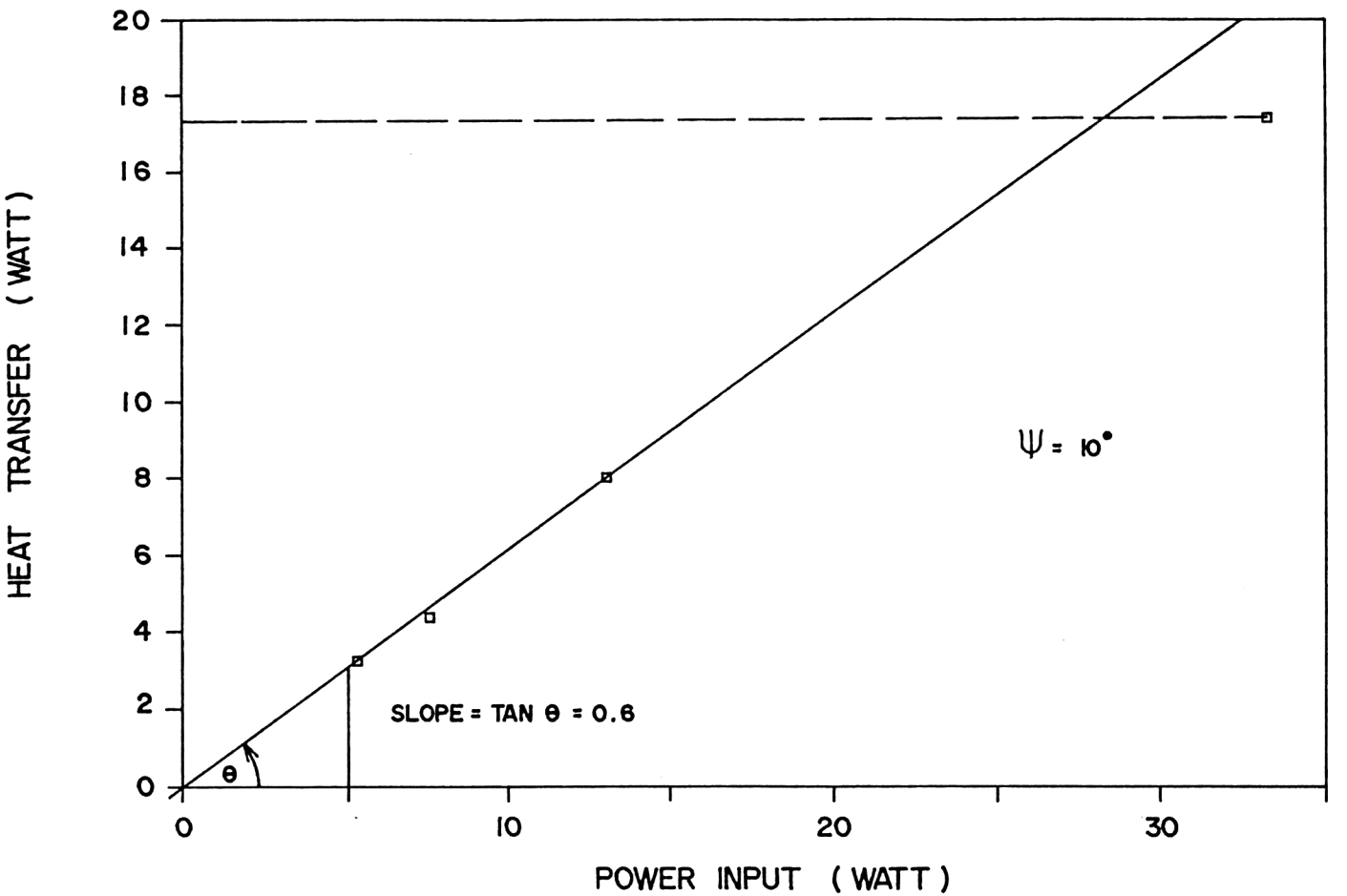

Fig. 4.22 Effect of Power Input to Heat Transfer Rate

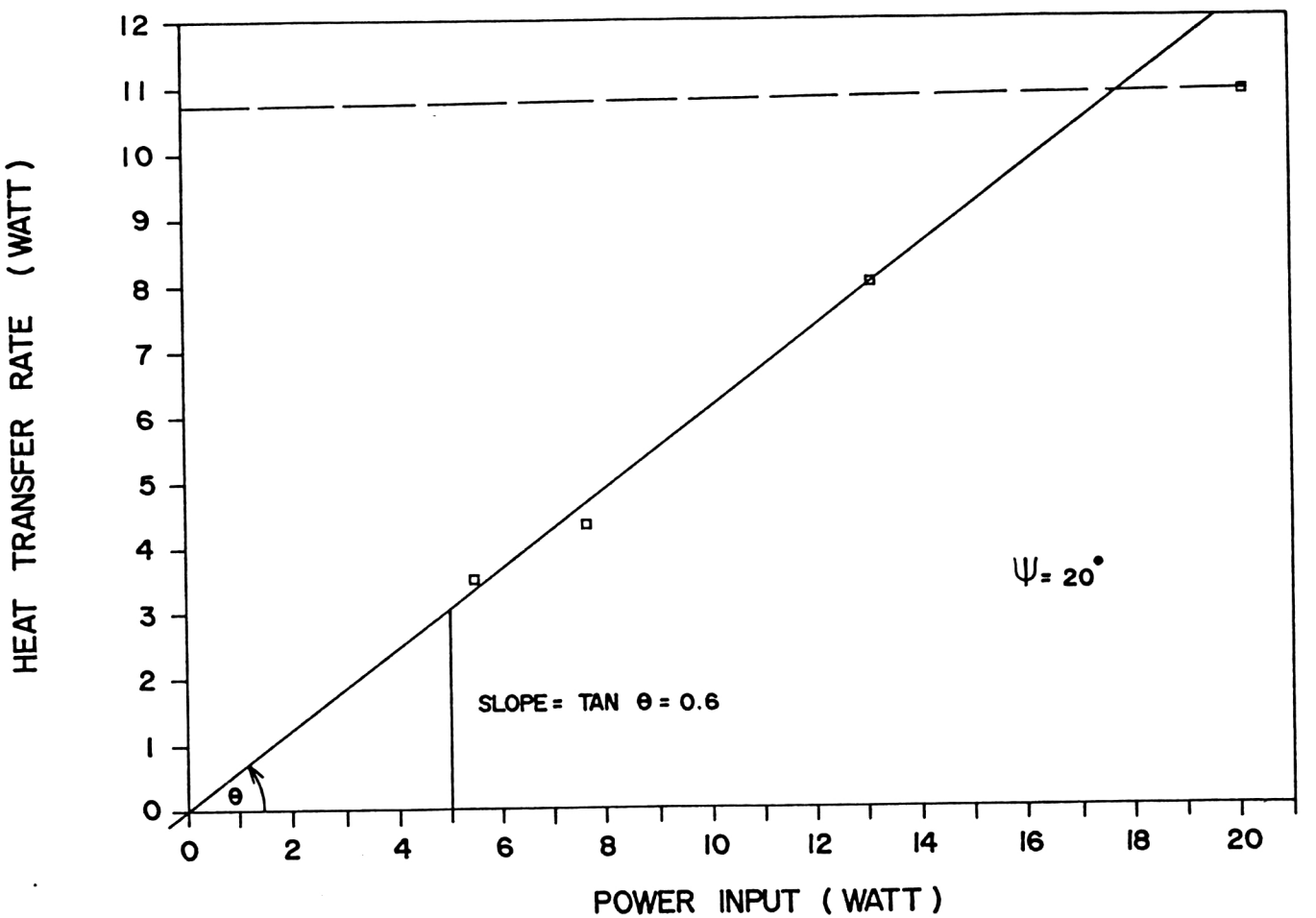

Fig. 4.23 Effect of Power Input to Heat Transfer Rate

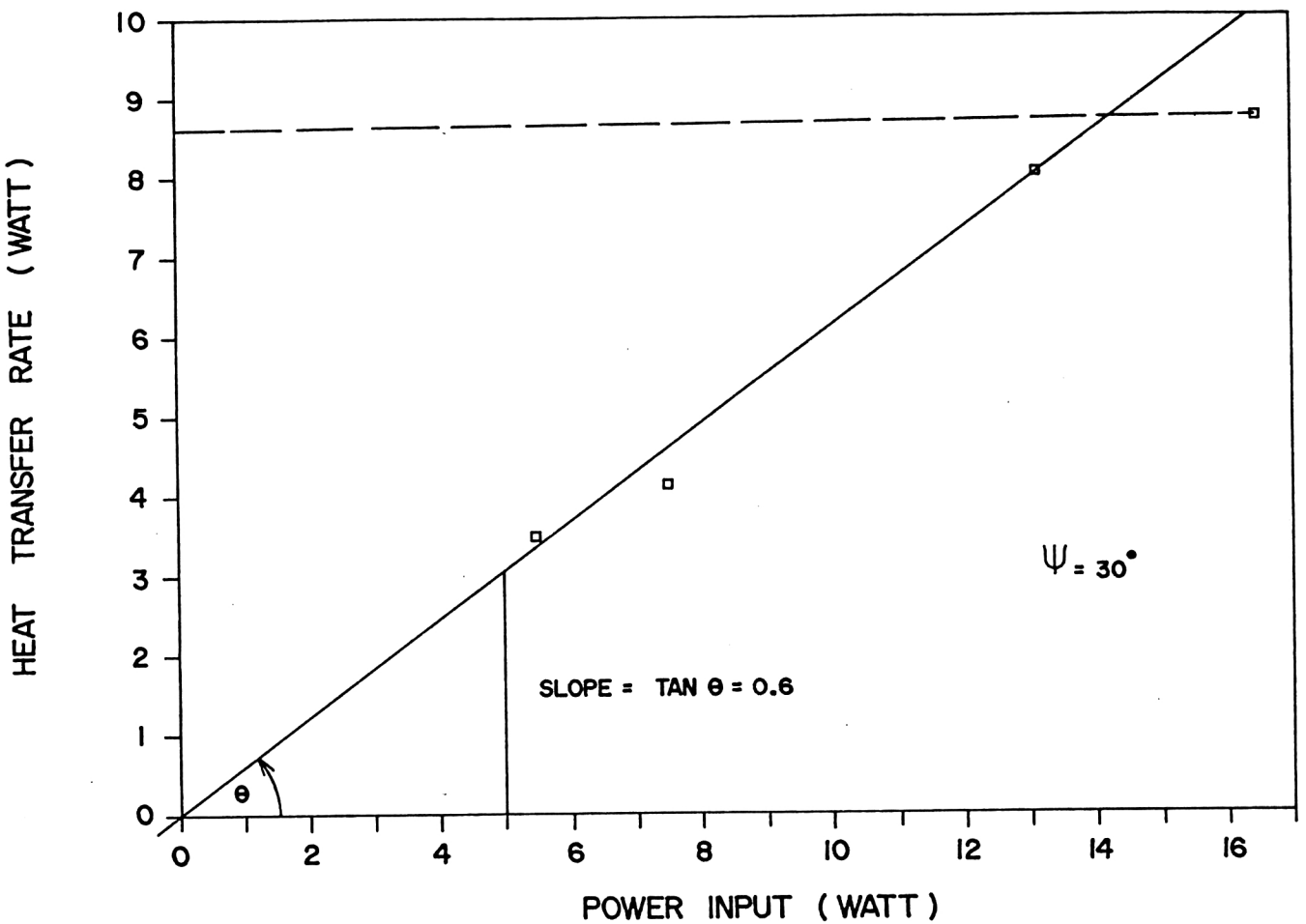

Fig. 4.24 Effect of Power Input to Heat Transfer Rate

Table 4.4 Effect of Heat Input on Heat Transfer Rate and Its Prediction (based on Fig. 4.17 to Fig. 4.21)

θ (DEGREES)	HEAT INPUT (WATTS)	HEAT TRANSFER RATE		RELATIVE ERROR (%)
		EXPERIMENT (WATTS)	ANALYSIS (WATTS)	
10	5.34	3.32	3.204	3.49
	7.58	4.34	4.548	4.79
	13.08	8.04	7.848	2.38
20	5.42	3.58	3.252	9.16
	7.6	4.36	4.56	4.58
	13.06	8.04	7.836	2.53
30	5.45	3.53	3.27	7.36
	7.5	4.2	4.5	7.14
	13.12	8.04	7.872	2.08